

1 Estimation of mechanistic parameters in the gas-phase reactions of 2 ozone with alkenes for use in automated mechanism construction

3 Mike J. Newland^{1,a}, Camille Mouchel-Vallon^{1,b}, Richard Valorso², Bernard Aumont², Luc
4 Vereecken³, Michael E. Jenkin⁴, Andrew R. Rickard^{1,5}

5 ¹ Wolfson Atmospheric Chemistry Laboratories, Department of Chemistry, University of York, United Kingdom

6 ² Univ Paris Est Creteil and Université de Paris, CNRS, LISA, F-94010 Créteil, France.

7 ³ Forschungszentrum Jülich GmbH, Institute for Energy and Climate, IEK-8 Troposphere, 52428 Jülich, Germany

8 ⁴ Atmospheric Chemistry Services, Okehampton, Devon, EX20 4QB, United Kingdom.

9 ⁵ National Centre for Atmospheric Science, Wolfson Atmospheric Chemistry Laboratories, University of York,
10 United Kingdom.

11
12 ^a now at: ICARE-CNRS, 1 C Av. de la Recherche Scientifique, 45071 Orléans Cedex 2, France.

13 ^b now at: Laboratoire d'Aérodologie, Université de Toulouse, CNRS, UPS, Toulouse, France.

14 *Correspondence to:* Mike Newland (mike.newland@gmail.com) and Andrew Rickard
15 (andrew.rickard@york.ac.uk).
16

17 **Abstract.** Reaction with ozone is an important atmospheric removal process for alkenes. The ozonolysis reaction
18 produces carbonyls, and carbonyl oxides (Criegee intermediates, CI), which can rapidly decompose to yield a
19 range of closed shell and radical products, including OH radicals. Consequently, it is essential to accurately
20 represent the complex chemistry of Criegee intermediates in atmospheric models in order to fully understand the
21 impact of alkene ozonolysis on atmospheric composition. A mechanism construction protocol is presented which
22 is suitable for use in automatic mechanism generation. The protocol defines the critical parameters for describing
23 the chemistry following the initial reaction, namely: the primary carbonyl / CI yields from the primary ozonide
24 fragmentation; the amount of stabilisation of the excited CI; the unimolecular decomposition pathways, rates and
25 products of the CI; the bimolecular rates and products of atmospherically important reactions of the stabilised CI
26 (SCI). This analysis implicitly predicts the yield of OH from the alkene-ozone reaction. A comprehensive database
27 of experimental OH, SCI and carbonyl yields has been collated using reported values in the literature and used to
28 assess the reliability of the protocol. The protocol provides estimates OH, SCI and carbonyl yields with a root
29 mean square error of 0.13 and 0.12 and 0.14, respectively. Areas where new experimental and theoretical data
30 would improve the protocol and its assessment are identified and discussed.

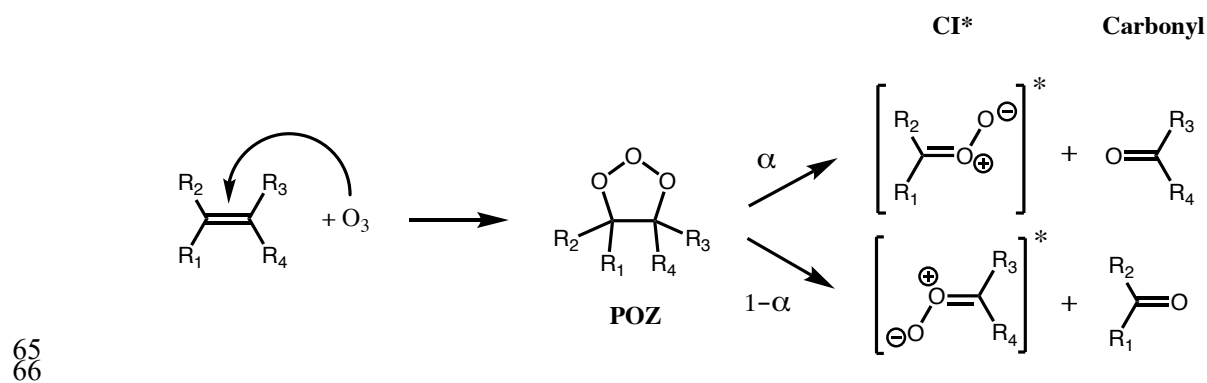
31 1 Introduction

32 Reaction with ozone is an important atmospheric removal process for alkenes, competing with reaction with OH
33 and NO₃ radicals. The ozonolysis reaction produces carbonyls and carbonyl oxides, commonly denoted Criegee
34 intermediates (CI), which can rapidly rearrange or decompose to yield a range of closed shell and radical products
35 (Johnson and Marston, 2008). Alkene ozonolysis has been shown to be an important non-photolytic source of OH
36 radicals, with field measurements (Paulson and Orlando, 1996; Elshorbany et al., 2009) and modelling studies
37 (e.g. Bey et al., 1997) suggesting it to be the dominant tropospheric OH source at night, in the winter (Heard et
38 al., 2004; Emmerson et al., 2005), and in indoor environments (Carslaw, 2007). Unimolecular CI reactions (Ehn
39 et al. 2014; Iyer et al., 2020) and bimolecular reactions of Stabilised Criegee Intermediates (SCI), with e.g. organic
40 acids and peroxy radicals (e.g. Kristensen et al., 2014; Sakamoto et al., 2013; Zhao et al., 2015; Mackenzie-Rae

41 et al., 2016), have been implicated in secondary organic aerosol formation. SCI can also act as an oxidant, this
 42 has been studied particularly for the reaction with SO₂ (e.g. Welz et al., 2012, Mauldin et al., 2012; Caravan et al.,
 43 2020) which can lead to sulfate aerosol production and hence impact radiative forcing and climate (Pierce et al.
 44 2013; Percival et al. 2013). However, both the SO₂ and organic acid reactions, while important locally, are likely
 45 only of minor importance to global budgets of sulfate aerosol and organic acids (Welz et al., 2014; Newland et
 46 al., 2018). The dominant removal processes for most SCI in the troposphere are reaction with water vapour or
 47 unimolecular reaction (Vereecken et al., 2017). However, for certain structures, these reactions are sufficiently
 48 slow for bimolecular reactions with other trace gases to become important.

49 Understanding of the complex nature of the chemistry of Criegee intermediates has progressed rapidly
 50 in recent years, particularly with regard to the mechanisms and rates of decomposition of CI (i.e. SCI and
 51 chemically excited CI (CI*)), and the bimolecular reaction rates of SCI. This has been facilitated by: direct
 52 experimental measurements of CI kinetics, generating CI through photolysis of di-iodo precursors (e.g. Welz et
 53 al., 2012; Chhantyal-Pun et al. 2020, and references therein); indirect measurements of CI kinetics during alkene
 54 ozonolysis experiments (e.g. Berndt et al. 2014a, 2014b, 2015; Newland et al., 2015), and extensive theoretical
 55 studies (e.g. Vereecken et al., 2017, and references therein).

56 The reaction of ozone with alkenes proceeds by a concerted addition to the C=C double bond, forming a
 57 short lived Primary Ozonide (POZ). Typically, the POZ fragments into two pairs of carbonyls and Criegee
 58 intermediates (CI) (Figure 1); for small to medium sized alkenes (C_{≤10}) this POZ is vibrationally excited,
 59 decomposing promptly, while for large alkenes (e.g. C_{≥15}, sesquiterpenes), theoretical studies suggest that the POZ
 60 can be collisionally stabilized prior to decomposition (Chuong et al., 2004; Nguyen et al., 2009a). Theoretical
 61 work also indicates that a small fraction of the POZ can rearrange to a carbonyl-hydroperoxide when vinylic H-
 62 atoms are present (Pfeifle et al., 2018); this mechanism is discussed separately below. It has also been suggested
 63 that different pathways may play a more significant role for a small number of systems e.g. cyclohexadienes
 64 (Pinelo et al., 2013).



67 **Figure 1. First step of alkene ozonolysis. A primary ozonide (POZ) is formed which rapidly decomposes to yield a pair**
 68 **of chemically activated Criegee intermediates and carbonyl products.**

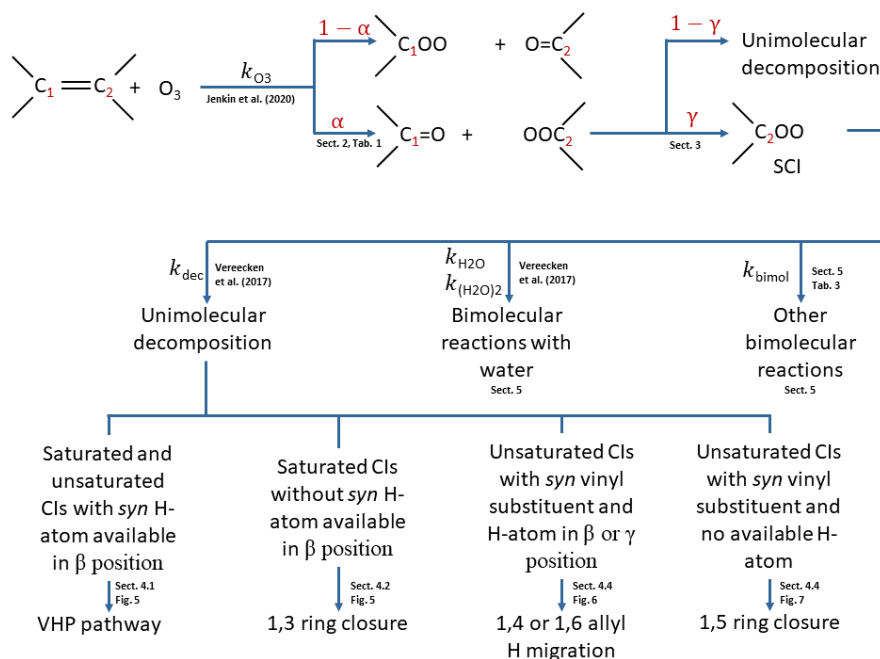
69 Criegee intermediates are generally zwitterionic in nature, as shown in Figure 1, but the moiety is denoted
 70 simply as a >COO structure below (not to be confused with alkylperoxy radicals, ROO[•]). CI can be formed with
 71 the terminal oxygen of the carbonyl oxide moiety in either an *E* (*anti*) or *Z* (*syn*) configuration relative to a given
 72 substituent group. The two conformers are not in rapid equilibrium, with quantum calculations showing that the
 73 energy barrier to rotational interconversion for CH₃CHOO is about 210 kJ mol⁻¹ (Johnson and Marston, 2008, and
 74 references therein); this was confirmed by Vereecken et al. (2017) who calculated barriers exceeding 120 kJ mol⁻¹

75 ¹ for saturated CI conformers. Isomeric CI conformers have been shown to have different unimolecular reaction
76 rates (e.g. Vereecken et al., 2017), follow different unimolecular pathways (Herron and Huie, 1977; Niki et al.,
77 1987; Martinez and Herron, 1987; Kidwell et al., 2016), and have very different reaction rates with water (e.g.
78 Taatjes et al., 2013; Sheps et al., 2014; Huang et al., 2015). Therefore, these conformers must necessarily be
79 considered as separate species, irreversibly partitioned according to their nascent ratios, to accurately represent
80 the effects of alkene ozonolysis on atmospheric composition.

81 Structure Activity Relationships (SARs) are commonly used to design the protocols needed to develop
82 automated mechanism generation tools (Vereecken et al., 2018). This paper forms part of a series of articles
83 devoted to the development of SARs for mechanism generation (Jenkin et al., 2018a, 2018b, 2019, 2020). Updated
84 SAR methods for the initial reactions of O₃ with unsaturated organic compounds are presented in a companion
85 paper (Jenkin et al., 2020), while in this work, a protocol is presented for the subsequent chemistry occurring
86 following the initial O₃ addition. This protocol details the yields of carbonyls and Criegee intermediates from the
87 alkene + O₃ reaction, and the subsequent fate of the Criegee intermediates, and accounts for the minor pathway
88 by carbonyl-hydroperoxide radical formation. The protocol is based on available experimental data and theoretical
89 data combined. For areas in which limited data exists, the protocol is set up to be easily updated as new
90 experimental or theoretical results become available. These areas are highlighted in the paper and are
91 recommended areas of further research. The protocol is currently being used to guide development of alkene
92 ozonolysis chemistry in the Generator for Explicit Chemistry and Kinetics of Organics in the Atmosphere,
93 GECKO-A (Aumont et al., 2005), and the Master Chemical Mechanism, MCM (Jenkin et al., 1997, Saunders et
94 al., 2003). It is noted that the protocol does not currently consider aromatic species that have been shown to react
95 with ozone, such as catechols, for which the mechanism may be different to the Criegee mechanism described
96 here.

97 The methodology for applying the protocol described in this work is summarised in Figure 2. The initial
98 addition of ozone to the double bond follows the protocol described in the companion paper (Jenkin et al., 2020).
99 The POZ formed from this protocol then decomposes according to the rules determined in Section 2, to give the
100 primary carbonyl and the CI yields (α), and possibly a minor fraction of carbonyl-hydroperoxide. A fraction (γ)
101 of the CI is then stabilised (Section 3). Both the stabilised and chemically activated CI then follow the relevant
102 set of rules from Vereecken et al. (2017) to ascribe them unimolecular decomposition mechanisms (and hence
103 products) and rates (Section 4), and bimolecular reaction rates with water vapour (Section 5). Finally, bimolecular
104 reaction rates with other atmospherically important species are assigned as a function of the SCI structure (Section
105 5).

106



107

108 **Figure 2. Flow diagram for implementation of the protocol. α = branching ratios in POZ decomposition, γ = fraction**
 109 **of CI stabilised. >COO denotes the Criegee intermediate formed.**

110 2 Primary Ozonide Fragmentation

111 2.1 Alkenes with aliphatic substituents

112 The fragmentation of the POZ has previously been parameterized based on the branching pattern around the
 113 double bond of the parent alkene (Jenkin et al., 1997; Rickard et al., 1999). Generally, it can be said that there is
 114 a preference for formation of the more substituted CI, e.g. the ozonolysis of 2-methyl propene yields ~ 0.7
 115 $(CH_3)_2COO$ and $\sim 0.3 CH_2OO$ (Rickard et al., 1999). However, consideration of just the immediate substituents
 116 of the double bond breaks down for more complex structures and for oxygenated substituents. There is clearly
 117 also an effect of substitution around the carbon adjacent to the double bond (the α -carbon atom). For instance,
 118 when there is a *t*-butyl group attached to the double bond, a strong preference is seen for formation of the opposing
 119 CI, as observed for yields of trimethylacetaldehyde from 3,3-dimethyl-1-butene (0.67) and trans-2,2-dimethyl-3-
 120 hexene (0.84) (Grosjean and Grosjean, 1997a). Using data from Grosjean and Grosjean (1997a), various
 121 homologous series of alkenes can be considered, such as the series with increasing methyl substitution on the α -
 122 carbon. For the 1-alkene series (Figure 3), yields of the larger carbonyl of 0.35, 0.51, and 0.67 are determined for
 123 1-butene, 3-methyl-1-butene, 3,3-dimethyl-1-butene respectively.

124

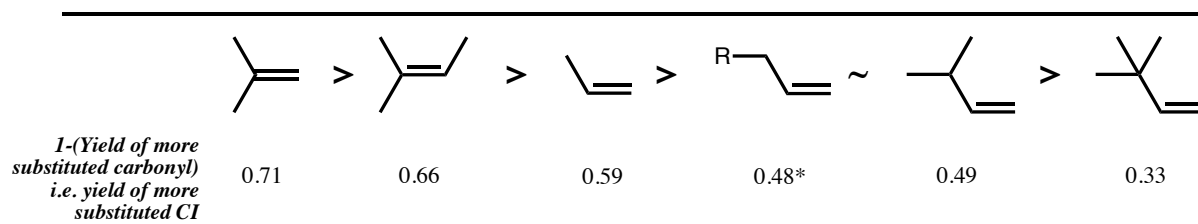


Figure 3. Decreasing order of preference, from left to right, of more substituted CI formation from ozonolysis of example alkyl substituted alkenes. Values are 1 – (mean of measured yields of carbonyls) (Spreadsheet S1). * Mean measured yield of propanal (i.e. 1 – more substituted CI) formation from 1-butene is 0.35, but for all other 1-alkenes the yield of the larger primary carbonyl product ranges from 0.45 – 0.50.

Such relationships have been observed and discussed previously by Grosjean and Grosjean (1997a) in terms of: (i) steric hindrance potentially weakening the O-O bond in the POZ on the side of the bulky substituent, and (ii) the inductive effect of adjacent alkyl groups strengthening the O-O bonds in the POZ (Grosjean and Grosjean, 1997a). Earlier work considering POZ fragmentation in the aqueous phase (Fliszár and Renard, 1970; Fliszár and Granger, 1970; Fliszár et al., 1971) described similar relationships to those observed in the gas phase (i.e. that shown in Figure 3), except in the case of terminal alkenes, for which the reverse trend was observed. In these studies, the observed trends are discussed in terms of stabilisation of the positive charge on the carbon in the POZ through: (i) ‘hyperconjugative stabilisation’ in the transition state, and (ii) the inductive effect during the POZ cleavage, with steric effects discounted as being unimportant in determining the POZ fragmentation pattern. Finally, Vereecken et al. (2017, Table 16 in the supplementary material) analysed the stability of CI in terms of group additivity factors, showing that alkyl-substituted CI are more stable than H-substituted CI, but where the stability of the CI is inversely proportional to the branching on the β -carbon atom.

These works can be summarised by saying that it appears that a substituent with a partial negative charge, such as a methyl group, can stabilise the positive charge on the adjacent carbon in the POZ. This leads to a greater yield of the CI containing the more stabilising substituents. On the other hand, a substituent that leads to a partial positive charge on the α -carbon leads to a lower yield of that CI.

2.2 Oxygenated alkenes

Following the rationale discussed above, oxygenated substituents on the α -carbon might be expected to strongly influence the primary ozonide fragmentation pattern. The number of product yield studies on the ozonolysis of most classes of unsaturated oxygenates is rather limited. As discussed below, some oxygenated substituents appear to destabilise the positive charge on the carbon in the POZ (i.e. disadvantaging POZ fragmentation towards the production of the CI on the oxygenated side), particularly carbonyl groups, while others such as acrylate esters and carboxylic acids may stabilise the CI, favouring its formation. However, data is very limited and often ambiguous for most of the oxygenated classes. This is partly due to challenges in measuring products containing multiple oxygenated groups, partly that some of these classes are likely to be present in negligible amounts in the atmosphere and, for some, that ozonolysis will be a negligible atmospheric sink compared to e.g. reaction with OH or photolysis. The available data is provided in the Supplement, Spreadsheet S1.

2.2.1 Enones / enals

Primary carbonyl yields have been reported for two α - β terminally unsaturated ketones ($H_2C=CHC(O)R$). For methyl vinyl ketone (MVK), Grosjean et al. (1993) and Ren et al. (2017) determined a strong preference for

160 formation of the ketone substituted product methyl glyoxal (0.87 and 0.71 ± 0.06 (with no OH scavenger)
161 respectively). For ethyl vinyl ketone, primary carbonyl yields for formaldehyde (HCHO) and 2-oxobutanal have
162 been determined to be 0.55 and 0.44 (Grosjean et al., 1996), and 0.37 and 0.49 (Kalalian et al., 2020) respectively,
163 displaying no clear preference for either fragmentation pathway. For α - β unsaturated ketones ($R_1CH=CHC(O)R_2$),
164 Grosjean and Grosjean (1999) measured the primary carbonyl yields from ozonolysis of 4-hexen-3-one to be:
165 acetaldehyde (CH_3CHO), 0.51 ± 0.01 , and 2-oxobutanal ($CH_3CH_2C(O)CHO$), 0.56 ± 0.02 , while Wang et al. (2015)
166 measured the primary carbonyl yields from ozonolysis of 3-methyl-3-buten-2-one ($CH_2=CR_1C(O)R_2$) to be:
167 diacetyl ($CH_3COCOCH_3$) 0.30 ± 0.03 , and HCHO 0.44 ± 0.05 , and from 3-methyl-3-penten-2-one
168 ($R_1CH=CR_2C(O)R_3$), diacetyl 0.39 ± 0.04 and CH_3CHO 0.61 ± 0.07 . For ozonolysis of 2-enals, yields have been
169 reported for crotonaldehyde (2-butenal) (CH_3CHO 0.42, glyoxal 0.47) (Grosjean and Grosjean, 1997b) and trans-
170 2-hexenal (butanal 0.53, glyoxal 0.56) (Grosjean et al., 1996). For the atmospherically important isoprene
171 oxidation product methacrolein (2-methyl-prop-2-enal, MACR), Grosjean et al. (1993) measured yields of methyl
172 glyoxal of 0.58 ± 0.06 and HCHO of 0.12 ± 0.03 . For 2-ethyl acrolein, the ethyl glyoxal yield has been measured to
173 be 0.14 by Grosjean et al. (1994), and 0.49 ± 0.03 by O'Dwyer et al. (2010).

174 To summarise, the presence of a carbonyl group on a double bond appears to favour formation of the
175 opposing CI. However, this effect is neutralised to an extent by the presence of an alkyl substituent on the same
176 side of the double bond, e.g. in the case of 3-methyl-3-buten-2-one, methacrolein, and 2-ethyl acrolein. There
177 remain large uncertainties on the trends in these classes (it is noted that in some cases the sum of the measured
178 primary carbonyl yields is well below one). They clearly warrant further study, owing to the significance of these
179 classes of compounds in atmospheric chemistry (e.g. MACR and MVK from isoprene oxidation (Wennberg et al.,
180 2018)).

181 2.2.2 Enols / enol ethers

182 There has been very little experimental work on the atmospheric chemistry of enols due to difficulties in synthesis,
183 storage, and measurement of these compounds. However, two recent theoretical studies examined the ozonolysis
184 of enols. The first (Lei et al., 2020) on the simplest enol, vinyl alcohol (ethenol), suggested that formation of
185 $CH_2OO + HCOOH$ is strongly favoured ($\sim 78\%$). The second (Wang et al., 2020), on the complex ketene-enol
186 species 4-hydroxy-1,3-butadien-1-one, also suggests that formation of HCOOH and the corresponding CI is
187 strongly favoured (84%). By contrast, there have been several experimental studies on the product yields of the
188 reactions of enol ethers ($R_1-O-CR_2=CR_3R_4$) with ozone. Most studies (Thiault et al., 2002; Klotz et al., 2004;
189 Barnes et al., 2005; Zhou et al., 2006; Zhou, 2007; Al Mulla et al., 2010) have determined that the dominant POZ
190 decomposition channel yields the formate ($R_1-O-C(O)R_2$) and the corresponding CI (R_3R_4COO), with measured
191 yields of the formate ranging from 55% - 89% (see Spreadsheet S1). An exception to these studies is the work
192 of Grosjean and Grosjean (1997b; 1999), which tended to find similar yields of the two primary carbonyl products.

193 2.2.3 Esters / acids

194 The primary carbonyl products of ozonolysis of the acrylate esters: methyl acrylate, ethyl acrylate, and methyl
195 methacrylate were studied by Bernard et al. (2010). Grosjean and Grosjean (1997b) also studied methyl acrylate.
196 There is no clear evidence for a preferential route for POZ fragmentation in these studies (see Spreadsheet S1).
197 The primary carbonyl yields from vinyl acetate ozonolysis were measured to be 0.30 ± 0.04 and 0.70 ± 0.08 for

198 HCHO and $\text{CH}_3\text{C}(\text{O})\text{OC}(\text{O})\text{H}$ respectively by Al Mulla et al. (2010), and 0.20 ± 0.06 and 0.97 ± 0.08 by Picquet-
199 Varrault et al. (2010). These studies suggest a preference for formation of CH_2OO and the anhydride. There are
200 only two compounds reported for ozonolysis of α - β unsaturated acids: acrylic and methacrylic acid. For acrylic
201 acid ozonolysis in the presence of formic acid as an SCI scavenger, Al Mulla et al. (2010) measured yields of 1.48
202 ± 0.2 and < 0.1 for HCHO and $\text{HC}(\text{O})\text{C}(\text{O})\text{OH}$ respectively, while in the absence of formic acid that group
203 measured a yield of HCHO of 0.95 (Viero, 2008). For methacrylic acid, Al Mulla et al. (2010) measured yields
204 of 0.77 ± 0.07 and 0.74 ± 0.10 for HCHO and $\text{CH}_3\text{C}(\text{O})\text{C}(\text{O})\text{OH}$ respectively. It is difficult to rationalise these
205 results: the acrylic acid experiments suggest a preference for formation of the CI with the acid moiety, but the
206 methacrylic acid experiments suggest that the presence of a methyl group on the same side of the double bond as
207 the acid reduces this preference, in contrast to most other systems where methyl substitution increases the yield
208 of that CI. This is a recommended area for further study.

209 2.2.4 Alcohols

210 There are significant differences between measured primary carbonyl yields of α,β -unsaturated acyclic alcohols
211 between studies by Grosjean and Grosjean (1997b), Le Person et al. (2009), O'Dwyer et al. (2010) and Kalalian
212 et al. (2020). This is likely owing to different experimental setups between groups, and the difficulty of
213 quantitatively measuring compounds with multiple oxygenated substituents. Overall the data in Spreadsheet S1
214 suggest that the presence of a hydroxyl group in place of a hydrogen on the α -carbon may lead to a slight
215 preference for CI production on the other side of the double bond to the hydroxyl group.

216 2.3 Conjugated alkenes

217 The ozonolysis of conjugated alkenes leads to POZ with a vinyl substituent on the α -carbon. For non-symmetrical
218 conjugated alkenes, the measurement of primary carbonyl yields can only be used to determine the POZ
219 fragmentation if the relative contribution of reaction at each double bond to the overall reaction rate is known. For
220 ozonolysis of the atmospherically important biogenic alkene isoprene, the primary carbonyl yields recommended
221 by IUPAC (Atkinson et al., 2006; iupac-aeris.ipsl.fr, last accessed 6 December 2021) are: methyl vinyl ketone
222 (MVK), 0.17 ; methacrolein (MACR), 0.41 ; and HCHO 0.42 . Based on reported product yields, the contribution
223 of reaction to each double bond to the overall rate has been estimated to be 0.6 for the terminal double bond and
224 0.4 for the substituted double bond (Nguyen et al., 2016; Jenkin et al., 2020). However, to the authors' knowledge
225 there has been no direct measurement of the reaction at each double bond, and this represents a significant
226 uncertainty in one of the most important atmospheric ozonolysis systems. Based on this assumption, and the
227 recommended yields of MVK and MACR, the formation of $\text{MACR} + \text{CH}_2\text{OO}$ is favoured over methacrolein oxide
228 (MACRO) + HCHO, and there is a slight preference for formation of methyl vinyl ketone oxide (MVKO) +
229 HCHO compared to $\text{MVK} + \text{CH}_2\text{OO}$. The MACR channel would suggest that the vinyl substituent is less
230 favourable in the POZ decomposition compared to a hydrogen. The methyl group present in MVKO stabilises the
231 CI (see section 2.1), leading to a preference for this channel. For symmetrical alkenes, the primary carbonyl yields
232 should be directly representative of the POZ fragmentation. For 1,3-butadiene, an acrolein yield of $51 - 52\%$ has
233 been measured (Niki et al., 1983; Kramp and Paulson, 2000), suggesting little preference for either POZ
234 decomposition pathway, in contrast to the analogous MACR channel in isoprene. Lewin et al. (2001) reported
235 complementary carbonyl yields from ozonolysis at the internal bond of (*E*) and (*Z*)-penta-1,3-diene and 5-

236 methylhexa-1,3-diene, which all showed a preference for formation of the unsaturated carbonyl (i.e. the saturated
237 CI), suggesting that the vinyl group is less favourable than a methyl or isopropyl group, in agreement with the
238 observations from isoprene. Note that, once the unsaturated CI is formed, the vinyl group can conjugate with the
239 carbonyl oxide π -system, leading to additional stabilization such that vinyl-CI are more stable than H-substituted
240 CI (Vereecken et al. 2017); this is however a product-specific effect that is not available yet in the POZ
241 decomposition.

242 **2.4 Endocyclic alkenes**

243 Decomposition of the POZ formed in the ozonolysis of endocyclic alkenes, leads to a molecule containing both
244 the carbonyl oxide and carbonyl moieties. Thus for non-substituted cycloalkenes (e.g. cyclopentene) there is only
245 one possible CI that can be formed (which can be in either the *E* or *Z* configuration). This means that there are no
246 stable primary carbonyls formed and so the relative contributions of the POZ decomposition pathways cannot be
247 inferred from measured primary carbonyl yields as they can for aliphatic compounds. Even a simple endocyclic
248 system such as cyclohexene gives a complex range of gas-phase (Aschmann et al., 2003; Hansel et al., 2018) and
249 aerosol phase (Kalberer et al., 2000; Ziemann, 2002) products, which can be attributed to decomposition of both
250 the *E* and *Z* forms of hexanal carbonyl oxide. However, the measured OH yields can be used to give an estimate
251 of the amount of CI decomposing via the vinyl-hydroperoxide (VHP) pathway (see section 4.1). It is noted here
252 that it has been proposed that alternative unimolecular pathways (that do not yield OH) are available to the CI
253 formed from endocyclic alkenes (Chuong et al., 2004; Nguyen et al., 2009a; Long et al., 2019), but that these are
254 only dominant for stabilised CI. Since the stabilised CI yield is low for endocyclic alkenes, at least up to C₁₀
255 (monoterpenes) (Chuong et al., 2004), measured OH yields should give a fair representation of the relative amount
256 of CI decomposing via the VHP pathway). For non-substituted cycloalkenes, OH yields have been compiled by
257 Calvert et al. (2000) covering cyclo-pentene, -hexene, -heptene, -octene and -decene from a number of research
258 groups (Spreadsheet S2). There is some spread in the data but no clear evidence for favouring formation of *E* or
259 *Z* CI, i.e. OH yields tend to centre around ~0.5. For substituted cycloalkenes, Atkinson et al. (1995) measured an
260 OH yield of 0.90 for 1-methyl-1-cyclohexene, suggesting either that the dominant CI formed is the di-substituted
261 CI (which will then undergo decomposition via the VHP pathway to yield OH), or that the mono-substituted CI
262 is formed predominantly as the *syn* conformer. The former must be considered more likely based on the observed
263 trends in aliphatic alkenes for favouring formation of the more substituted CI, and that there appears to be little
264 preference for formation of *syn/anti*-CI from non-substituted endocyclic alkenes. 1-methyl-1-cyclohexene is
265 particularly important from the point of view of atmospheric chemistry as an analogue for the abundant biogenic
266 monoterpenes α -pinene and limonene. OH yields from α -pinene and limonene ozonolysis have been measured
267 by a number of groups and are also generally high (0.64-0.91) (Cox et al. 2020), similar to 1-methyl-1-
268 cyclohexene.

269 **2.5 Exocyclic alkenes**

270 For exocyclic alkenes in which the double bond is attached to the ring, e.g. β -pinene, the data suggests that POZ
271 fragmentation strongly favours formation of the ring containing CI. For the monoterpene β -pinene, the mean
272 measured yield of the C₉ carbonyl, nopinone, is 0.21 (Grosjean et al., 1993; Hakola et al., 1994; Rickard et al.,
273 1999; Yu et al., 1999; Winterhalter et al., 2000; Hasson et al., 2001b; Lee et al., 2006; Ma and Marston, 2008),

274 with theoretical work (Nguyen et al., 2009b) suggesting that some of this may be secondary and that the primary
275 yield could be even lower. The other two compounds with a terminal double bond attached to the ring for which
276 there are data are camphene (0.36 yield of C₉ carbonyl (Hakola et al., 1994; Hasson et al., 2001b)) and methylene
277 cyclohexane (0.19 yield of C₆ carbonyl (Hasson et al., 2001b)). For the monoterpene sabinene, which has a
278 terminal double bond attached to a C₅ and C₇ ring, the mean measured yield of the C₉ carbonyl, sabinaketone, is
279 0.44. This is considerably higher than from those compounds where the double bond is on a C₆ ring, probably
280 demonstrating the impact of ring strain on the POZ fragmentation. The monoterpene terpinolene has a
281 disubstituted double bond attached to a six membered ring. Reported yields of the ring containing carbonyl
282 (0.40±0.06 (Hakola et al., 1994); 0.40±0.08 (Reissell et al., 1999); 0.45 (Ma and Marston, 2009)) suggest yields
283 of the ring containing CI of 0.60 and 0.55 respectively; this assumes 100% reaction at the exocyclic double bond,
284 with Hakola et al. (1994) measuring a yield of ≤ 2 % of the dicarbonyl expected as a product (though by no means
285 the only one) from reaction at the endocyclic double bond. These CI yields are lower than for the exocyclic alkenes
286 with terminal double bonds, but are still considerably higher than most compounds which have a dimethyl
287 substitution on the double bond, for which acetone yields tend to be ~ 0.3. The presence of a ring clearly has a
288 different effect to simply having two alkyl groups attached to the double bond, leading to much higher yields of
289 the ring containing CI.

290 For alkenes with a vinyl group attached to a ring, there are data only for vinyl cyclohexane, and its aromatic
291 analogue styrene. These have similar yields for the ring containing carbonyl of 0.62 and 0.64 respectively
292 (Grosjean and Grosjean, 1997a). There is no data for alkenes with double bonds more distant from a ring.

293 2.6 Yields of CI stereo-conformers

294 The formation of *syn/anti* conformers of CI in alkene ozonolysis was first discussed by Bauld et al. (1968), to
295 explain the observed *cis/trans* yields of the secondary ozonide formed from ozonolysis in the aqueous phase. Their
296 observations suggested that ozonolysis of *cis*-alkenes will predominantly form *anti*-CI, while for *trans*-alkenes
297 the predominance was less clear and appeared to be dependent on alkene structure. In the gas phase, *but-2-ene* is
298 the most studied system. Various experimental work has observed higher yields of OH from *trans*-*but-2-ene*
299 compared to *cis*-*but-2-ene* (see Spreadsheet S3). Assuming that only (*Z*)-CI decomposition yields OH (see Section
300 4.1), this implies a higher nascent (*Z*):(*E*)-CH₃CHOO ratio from decomposition of the POZ formed in *trans*-*but*-
301 *2-ene* ozonolysis. Orzechowska and Paulson (2002) measured a ratio of 1.62 for the OH yields from *trans/cis*-
302 *but-2-ene*. They observed a similar relationship for *trans/cis*-*pent-2-ene* and *trans/cis*-*hex-3-ene*, with OH yield
303 ratios determined as 1.80 and 1.51 respectively. Assuming that OH comes exclusively from (*Z*)-CH₃CHOO
304 implies a (*Z*):(*E*)-RCHOO ratio of 0.60:0.40 – 0.64:0.36 for these three systems. Kroll et al. (2002) determined a
305 similar OH yield ratio for *trans/cis*-*hex-3-ene*, but using isotopically labelled hydrogen atoms demonstrated that
306 a fraction of this OH was not coming from the (*Z*)-CI. From their OH yield measurements, they inferred a (*Z*):(*E*)-
307 C₂H₅CHOO ratio of 50:50 for *trans-3-hexene*, and 20:80 for *cis-3-hexene*. Campos-Pineda and Zhang (2017)
308 reported direct measurements of the vinoxy radical formed in decomposition of *syn*-CH₃CHOO, from *cis*- and
309 *trans-but-2-ene* ozonolysis, inferring a yield of *syn*-CH₃CHOO of ~0.5 from *trans-but-2-ene* and ~0.3 from *cis*-
310 *but-2-ene*, broadly in line with estimations from measured OH yields.

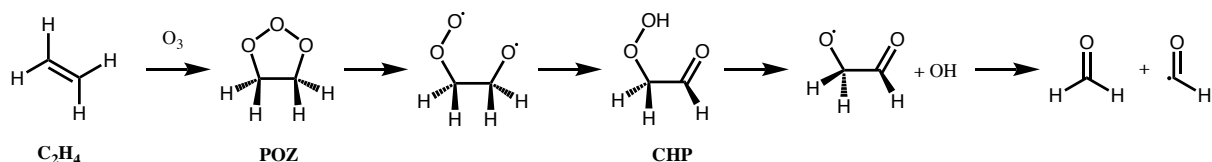
311 Early theoretical calculations considering the gas phase (Cremer, 1981a,b) suggested that (*Z*)-RCHOO is
312 likely to be formed in greater yield for small alkenes, but that (*E*)-RCHOO becomes more favoured in the

313 ozonolysis of large alkenes. Calculations by Rathman et al. (1999) suggested that (*Z*)-CH₃CHOO should be
314 favoured in *trans*-but-2-ene ozonolysis, but that conversely (*E*)-CH₃CHOO would be favoured in *cis*-but-2-ene
315 ozonolysis. Recent theoretical work (Watson, 2021) looking at POZ fragmentation for a series of disubstituted 2-
316 alkenes (CH₃CH=CHR), suggests formation of (*E*)-RCHOO will be strongly favoured in the ozonolysis of *cis*-
317 alkenes (87 % for *cis*-but-2-ene, increasing to 93 % for *cis*-2-hexene), while there is a roughly equal split from
318 ozonolysis of *trans*-alkenes. This is in qualitative agreement with the experimental work discussed above but
319 suggests a stronger preference than observed in the direct measurements of the vinyloxy radical by Campos-Pineda
320 and Zhang (2017). For tri-substituted alkenes, Watson (2021) finds a strong preference for formation of (*E*)-
321 RCHOO on the mono-substituted side of the double bond. For the C₄-CI formed in isoprene ozonolysis, theoretical
322 calculations have determined a relative split of 50:50 for the two conformers of MVKO (Kuwata et al., 2005), and
323 20:80 for *syn*-MACRO:*anti*-MACRO (Kuwata and Valin, 2008). This is in qualitative agreement with the
324 observed low OH yield (0.08-0.13) from 1,3-butadiene (Atkinson and Aschmann, 1993; Kramp and Paulson,
325 2000) if it is assumed that decomposition of *syn*-MACRO will have a high OH yield whereas *anti*-MACRO will
326 not yield OH. To the authors' knowledge there is no other information on the relative yields of *syn/anti*-R₁R₂COO
327 (where R₁ ≠ R₂).

328 2.7 POZ ring opening to a biradical

329 In addition to direct CI + carbonyl formation from the POZ, the possibility exists of ring opening of the POZ to a
330 singlet alkoxy-peroxy biradical (>C(O[•])-C(OO[•])<) (O'Neal and Blumstein, 1973; Olzmann et al., 1997; Anglada
331 et al., 1999; Fenske et al., 2000; Nguyen et al., 2015; Pfeifle et al., 2018) (Figure 4). In addition to re-closing the
332 ring to the POZ or decomposing to CI + carbonyl, this alkoxy-peroxy biradical can migrate an H-atom from the
333 alkoxy-bearing carbon, forming a carbonyl hydroperoxide (–C(=O)-C(OOH)<); this pathway is only possible if
334 the alkene has a vinylic H-atom. The carbonyl hydroperoxide formed has a high energy content, over 400 kJ mol⁻¹,
335 and can eliminate an OH radical, forming a α -carbonyl-alkoxy radical that rapidly decomposes to an acyl radical
336 and a carbonyl. This pathway has been invoked in theoretical studies as the main source of OH in the ozonolysis
337 of ethene (in which OH cannot be formed via a VHP) (Nguyen et al., 2015; Pfeifle et al., 2018), and is expected
338 to contribute somewhat to OH formation in other alkenes, though this has not yet been investigated experimentally
339 or theoretically. Alternative proposed sources of OH in ethene ozonolysis all involve the CH₂OO Criegee
340 intermediate. However, theory has shown that direct OH formation from CH₂OO by a 1,3-H-migration involves
341 too high a barrier (e.g. Nguyen et al., 2015; Pfeifle et al., 2018), while OH elimination from the hot formic acid
342 formed in the 1,3-ring closure (see Section 4.2) is not competitive against formation of H₂O + CO and H₂ + CO₂,
343 as also borne out by HCOOH pyrolysis experiments (Chang et al., 2007; Vichiatti et al., 2017). The carbonyl
344 hydroperoxide route thus resolves an apparent discrepancy between ethene ozonolysis experiments, which
345 observe significant OH yields, and experiments (Stone et al., 2018) and theoretical work (Nguyen et al., 2015;
346 Pfeifle et al. 2018), which indicate very little OH formation from CH₂OO. Pfeifle et al. (2018) calculated a yield
347 of 12.3 % for the carbonyl-hydroperoxide in ethene ozonolysis, while Nguyen et al. (2015) obtained 13 %, both
348 at the low end of the current IUPAC recommended OH yield (0.17±0.05) for the reaction (Cox et al., 2020).

349



353 **Figure 4. The carbonyl hydroperoxide (CHP) decomposition pathway for ethene ozonolysis**

354 2.8 Protocol Rules for POZ fragmentation

355 2.8.1 POZ fragmentation

356 A group contribution approach was designed to estimate POZ fragmentation yields. The approach assumes that
 357 the branching ratio for the two possible fragmentations of the POZ depends on the substituents of the
 358 $R_{1a}(R_{1b})C=C(R_{2b})R_{2a}$ parent alkene. The general form of the relationship is given by:

$$359 Y_{CI1} = \frac{(F_{1a}+F_{1b})-(F_{2a}+F_{2b})+1}{2} = 1 - Y_{CI2} \quad (E1)$$

360 where Y_{CI} is the CI production yield on the i^{th} carbon and F_R are the contributions for the 4 substituents on the
 361 C=C bond. The set of F_R values is developed based on the observed primary carbonyl yields (Supplementary
 362 Section S1 and Spreadsheet S1) and are based on a least squares fit to a relevant dataset of alkenes for each
 363 substituent (Figures S1-S5).

364 For a vinyl group, F is constrained to fit the IUPAC recommended yields of MVK and MACR from
 365 isoprene ozonolysis, assuming that ozone reacts 60% at the terminal double bond and 40% at the substituted
 366 double bond (Nguyen et al., 2016; Jenkin et al., 2020). The presence of a carbonyl group adjacent to the double
 367 bond appears to strongly favour formation of the opposing CI in the case of MVK (i.e. $-C(=O)CH_3$). However,
 368 this is not the case for other alkenes with the structure $-C(=O)R$ in the database, for which there appears to be no
 369 clear preference for formation of either CI, with a fit to the data yielding a slightly positive F value of 0.127. The
 370 strongest negative effect (i.e. most strongly favouring formation of the carbonyl containing the functional group)
 371 observed in the database is for enol ethers ($-OR$), giving an F value of -0.655. This is assumed to also be the same
 372 case for enols ($-OH$) based on the theoretical calculations of Lei et al. (2020) and Wang et al. (2020), and for vinyl
 373 esters ($-OC(=O)R$), based on the observed values for vinyl acetate. By contrast, an acrylate ester ($-C(=O)-OR$)
 374 substituent adjacent to the double bond does not appear to have a strong effect on fragmentation, and $F = 0$ is
 375 used. Similarly, the trend from the two unsaturated acids reported is unclear, and $F = 0$ is also used here. An OH
 376 group on the alpha carbon appears to slightly decrease Y_{CI} compared to an H atom, but the data is currently too
 377 limited to recommend a group additivity value, so the OH group is treated as an H atom, i.e. $F_{-CH_2OH} = F_{-CH_3}$.
 378 More distant oxygenated groups are not considered. The available data for exocyclic alkenes with the double bond
 379 attached to the ring is not able to take into account the effect of multiple rings, with F_{ring} being determined from
 380 only exocyclic alkenes with C₆ rings (β -pinene, methylene cyclohexane, and terpinolene). For rings with a vinyl
 381 group attached, $F_{(C_6)\text{ring}}$ is determined only from C₆ rings, i.e. styrene and vinylcyclohexane. Endocyclic alkenes
 382 are assumed to follow the same fragmentation patterns as acyclic alkenes. For example, cyclohexene is considered
 383 to have the structure $>CH_2CH_2CH=CHCH_2CH_2<$, 1-methyl cyclohexene $>CH_2CH_2C(CH_3)=CHCH_2CH_2<$ etc.

384 The group contribution value, F , is then used in Eq. (1) to determine the yield of CI₁ (defined as having
 385 substituents 1a and 1b) from the general structure R_{1a}(R_{1b})C=C(R_{2b})R_{2a}. Generally, the measurement of the larger
 386 primary carbonyl was used to determine the primary carbonyl and CI yields. This is because in some cases, the
 387 smaller carbonyl can be formed as a decomposition product of the larger CI and hence is not a true primary
 388 carbonyl yield.

389
 390
 391

Table 1. Group contribution values (F) for various substituents

<i>Group</i>	<i>Value</i>	<i>Alkenes used for fit</i>
=ring	+ 0.62	β-pinene, methylene cyclohexane, terpinolene
-CH ₃	+ 0.218	propene, 2-methyl butene, 2-methyl-but-2-ene
-C(=O)R, -C(=O)H	+ 0.127	2-ethylacrolein, ethyl vinyl ketone, 4-hexen-3-one, 3-methyl-3-buten-2-one, 3-methyl-3-penten-2-one, 2-butenal, trans-2-hexenal
-CH ₂ CH ₃	+ 0.107	but-1-ene, 2-methyl-but-1-ene, 2-ethyl-but-1-ene, 2,2-dimethyl-hex-2-ene
-H	0	By definition
-COOH, -C(=O)-O-R,	0	Acids and acrylate esters, see spreadsheet S1
-CH ₂ CH ₂ R	0	pent-1-ene, hex-1-ene, hept-1-ene, oct-1-ene, dec-1-ene, 2-methyl-pent-1-ene
-CHR ₁ R ₂	- 0.069	3-methyl-but-1-ene, 3-methyl-pent-1-ene, 2,3-dimethyl-but-1-ene, 2,4-dimethyl-pent-2-ene, 2,3,4-trimethyl-pent-2-ene, 3-methyl-2-isopropyl-but-1-ene
-(C ₆)ring	- 0.25	styrene, vinyl cyclohexane
-vinyl	- 0.28	isoprene
-CR ₁ R ₂ R ₃	- 0.386	2,3,3-trimethyl-but-1-ene, 2,4,4-trimethyl-pent-2-ene, 2,2-dimethyl-hex-3-ene, 3,3-dimethyl-but-1-ene
-OR, -OH, -OC(=O)R	- 0.655	methyl vinyl ether, ethyl vinyl ether, propyl vinyl ether, butyl vinyl ether, ethyl propenyl ether

392 2.8.2 *E/Z* conformer yields

393 In light of the current paucity of experimental and/or theoretical information on the relative yields, an equal 0.5:0.5
 394 yield is assigned as a default value for (*E*)/(*Z*) isomers for all asymmetrical CI. The following two exceptions are
 395 nevertheless considered. For acyclic *cis*-RCH=CHR parent alkenes, a relative yield of 0.7:0.3 is set for (*E*):(*Z*) CI.
 396 For conjugated structures, formation of (*E*)/(*Z*)->C=C(R)-CHOO is assumed to be in a ratio of 0.8:0.2, based on
 397 the work of Kuwata et al. (2005) and Kuwata and Valin (2008).

398 2.8.3 Carbonyl-hydroperoxide route

399 While there is little information available on the stepwise carbonyl-hydroperoxide POZ decomposition
 400 mechanism, it is needed to account for the radical yields observed in the ozonolysis of ethene as discussed above.
 401 There is no reason to assume it will not occur more generally for any alkenes with vinylic H-atom(s), though
 402 perhaps with different fates of the intermediate biradical and/or carbonyl hydroperoxide (e.g. larger
 403 hydroperoxides could be more prone to collisional stabilisation and yield less prompt OH). Currently this channel
 404 is only included for the ethene-ozone reaction, for which it is assumed that 0.12 of the ethene-ozone reaction
 405 forms the biradical intermediate, rather than the CI + carbonyl, using the contribution calculated for the carbonyl
 406 hydroperoxide channel by Pfeifle et al. (2018). When more general data become available, assuming the channel
 407 is active for other systems, the protocol will be updated. The general structure of such a scheme might be: the
 408 POZ is assumed to break either of the O-O bonds with equal probability, forming one of two possible biradicals.
 409 If there is an available vinyl α-hydrogen, it is assumed that the H-shift to the peroxy radical occurs, forming the
 410 carbonyl-hydroperoxide (R₁R₂C(OOH)C(=O)R₃), followed by loss of OH and scission of the C-C bond to yield

411 the stable product $R_1R_2C=O$ and the radical $R_3C^{\bullet}=O$. If there is no available α -hydrogen, the biradical is assumed
412 to yield the CI and carbonyl, either by C–C fragmentation or recyclisation to the POZ.

413 **3 Stabilisation of the Criegee Intermediate**

414 **3.1 Excited vs. stabilised CI**

415 Following decomposition of the primary ozonide, CI are formed with a broad range of internal energies (e.g.
416 Drozd et al., 2011). Consequently, it is often useful to consider the mean energy of a population of CI. Those
417 generated with a high internal energy, allowing prompt chemical reactions, are called excited, or chemically
418 activated CI (CI*). Those without enough internal energy to undergo prompt decomposition are considered to be
419 ‘stabilised’ CI (SCI). Additionally, CI* can be collisionally stabilised. This has been demonstrated by
420 experimental work showing that SCI yields are pressure dependent (Drozd et al., 2011, Hakala and Donahue,
421 2016; 2018). Note that this pressure dependence is moderate, and across the range of relevant atmospheric
422 pressures not of primary concern; we base our analysis on the available data near 1 atm.

423 **3.2 SCI Yield**

424 The total SCI yield for a given alkene is the sum of the fraction of the nascent CI population that is formed
425 stabilised, plus the fraction of CI* that is collisionally stabilised. The fate of the CI* is a competition between
426 prompt unimolecular decay and collisional stabilisation, with the CI* having a lifetime on the order of
427 nanoseconds against either of these processes (e.g. Drozd et al., 2017; Stephenson and Lester, 2020). Most alkenes
428 will form a number of different CI*, each with different lifetimes against unimolecular decay and collisional
429 stabilisation. The rate of collisional stabilisation of a given CI* is dependent on the frequency of collisions (and
430 hence pressure), and the efficiency of energy loss to the bath gas. The rate of unimolecular decay of a given CI*
431 depends on: (i) the energy of the CI* when formed, (ii) the activation energy for the most facile decay process /
432 the energy required for tunnelling, and (iii) the relative density of states of the reactants and transition state, i.e.
433 the entropy of the reaction. The dominant unimolecular decay mechanism is dependent on the structure of the CI;
434 these mechanisms are discussed in Section 5.

435 Larger CI* will tend to be stabilised to a greater extent due to a greater density of states distributing the
436 excess internal energy over a greater number of modes and so reducing the rate of unimolecular decay (Drozd and
437 Donahue, 2011; Stephenson and Lester, 2020). Hence, as the size of the CI increases relative to the carbonyl co-
438 product formed in POZ decomposition, the fraction of the energy taken by the CI from the POZ will increase
439 somewhat (assuming the energy has time to become equally distributed throughout the POZ), but typically the
440 mean excess energy per degree of freedom of the nascent CI population decreases, and hence the fraction of CI*
441 with enough energy to undergo unimolecular decay also decreases (Fenske et al., 2000; Newland et al., 2020).
442 This will lead to greater stabilisation. i.e. higher SCI yields. Similarly, for a given CI size, carbonyl co-products
443 of increasing size will take a larger fraction of the excess energy, leaving the CI* moiety with less energy and thus
444 will also lead to higher SCI yields (Newland et al., 2020). Conversely, for endocyclic alkenes, decomposition of
445 the POZ produces a single molecule containing both the carbonyl and carbonyl oxide moieties. Such CI have a
446 high initial energy, with no energy lost from the POZ decomposition to the carbonyl or to relative motion of the
447 fragments, and thus require many collisions to be quenched (Vereecken and Francisco, 2012). Consequently,

448 endocyclic alkenes with $\leq C_7$ have little stabilisation (Hatakeyama et al., 1984; Campos-Pineda and Zhang, 2017;
 449 Drozd and Donahue, 2011). For the endocyclic C_{10} monoterpenes α -pinene and limonene, total SCI yields have
 450 been measured to be 0.13-0.22 (Hatakeyama et al., 1984; Taipale et al., 2014; Sipilä et al., 2014; Newland et al.,
 451 2018) and 0.23-0.27 (Sipilä et al., 2014; Newland et al., 2018) respectively. For the C_{15} sesquiterpene β -
 452 caryophyllene, a total SCI yield (including from decomposition of the stabilised POZ) of 0.74 was calculated by
 453 Nguyen et al. (2009), with a value of > 0.6 determined experimentally (Winterhalter et al., 2009).

454 Total SCI yields have been measured experimentally for many alkene-ozone systems. These are generally
 455 determined indirectly, by performing ozonolysis experiments in the presence of an SCI scavenging species (e.g.
 456 H_2O , SO_2 , hexafluoroacetone). Measurements of scavenger removal, or formation of products from the SCI +
 457 scavenger reaction, are used to determine the SCI yield. Yields measured in such a way must be considered to be
 458 lower limits since, under most experimental conditions, a significant fraction of the SCI may undergo
 459 unimolecular decomposition based on recently reported fast SCI decomposition rates (e.g. Newland et al., 2015;
 460 Vereecken et al., 2017; Newland et al., 2018). The choice of scavenger species is also important. In some older
 461 experimental studies, water was used as an SCI scavenger, with H_2O_2 (e.g. Hasson et al., 2001a) or hydroxymethyl
 462 hydroperoxide (HMHP, e.g. Hasson et al, 2001a; Neeb et al., 1997) being the detected reaction products. For
 463 mono-substituted (*E*)-SCI, or for CH_2OO , this may be a reasonable assumption, with $k_{(H_2O+SCI)}[H_2O]/k_{(decomp.)} \sim$
 464 $10^2 - 10^3$ at $[H_2O] = 5 \times 10^{17} \text{ cm}^{-3}$ (e.g. Vereecken et al., 2017). However, for (*Z*)-SCI, $k_{(H_2O+SCI)}[H_2O]/k_{(decomp.)} \sim$
 465 $10^{-2} - 10^{-1}$, i.e. the majority of the SCI will not be scavenged by H_2O .

466 3.3 Protocol Rules for CI Stabilisation

467 The relationship between stabilisation of the CI^* and size of the carbonyl co-product has been studied for CH_2OO
 468 and $(CH_3)_2COO$ by Newland et al. (2020) (Figure 5). For CH_2OO this relationship might be expected to represent
 469 a minimum for CI^* that primarily decay via the 1,3 ring closure pathway (i.e. *anti*- CI^* , see Section 4.2), since
 470 larger CI^* will have a slower decay rate due to a greater density of states. Similarly, the trend for $(CH_3)_2COO$ can
 471 be assumed to be close to a minimum for CI^* that primarily undergo the 1,4 vinylhydroperoxide (VHP)
 472 decomposition pathway (see Section 4.1), with only *syn*- CH_3CHOO likely to have a lower density of states (and
 473 therefore faster decomposition) (Stephenson and Lester, 2020). With no further data available, the stabilisation
 474 trend of CH_2OO is used for CI^* that decompose via 1,3 ring closure, while that of $(CH_3)_2COO$ is used for CI^* that
 475 decay via the 1,4 vinylhydroperoxide pathway. For other pathways, such as the 1,5-ring closure to a dioxole (see
 476 Section 4.4), important in isoprene ozonolysis, no information is available. CI^* with a vinyl group *syn* to the
 477 terminal oxygen of the carbonyl oxide are considered as *syn*-CI for the purposes of calculating stabilisation in the
 478 protocol.

479 An extension of Equation E7 in Newland et al. (2020) is used to estimate the CI stabilisation S :

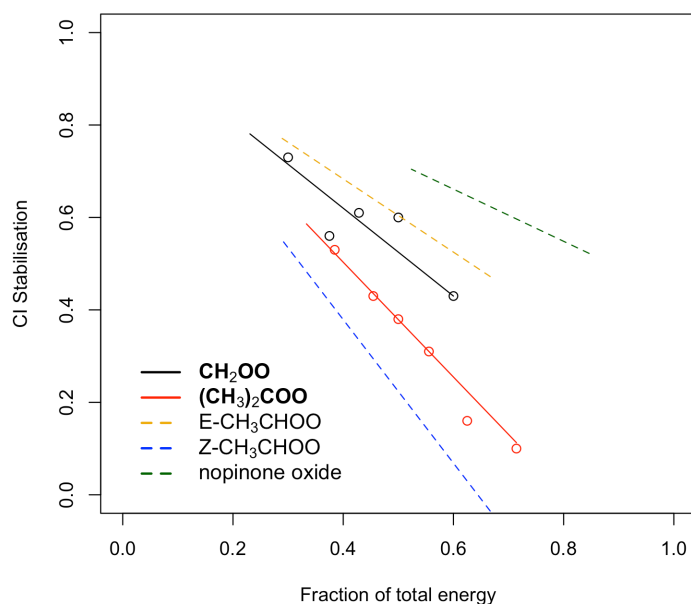
480

$$481 \quad S = 1 - \left[\left(\frac{A_{CI}}{A_{tot}} \right) \times F \times z_{path} \right] \quad (E2)$$

482 where A_{CI} is the total number of non-hydrogen atoms in the CI^* and A_{tot} is the total number of non-hydrogen atoms
 483 in the POZ. F_{13RC} and F_{VHP} are values determined for CH_2OO and $(CH_3)_2COO$, based on the SCI yields for their
 484 symmetrical parent alkenes ethene and 2,3-dimethylbut-2-ene, respectively. For CH_2OO this is 0.95 and for
 485 $(CH_3)_2COO$ it is 1.24 (Newland et al., 2020). In this work, an additional term, z_{path} , is included to take into account

486 the observed / predicted increased stabilisation of CI* with size. For CI* that decay via the 1,3 ring closure
 487 pathway, z_{13RC} is defined as $x / (A_{CI} + (x - A_{CH_2OO}))$, where A_{CH_2OO} is the total number of non-hydrogen atoms in
 488 CH_2OO (i.e. 3), and x is an adjustable parameter. For CI* that decay via the 1,4 H-shift, z_{VHP} is defined as $x / (A_{CI}$
 489 $+ (x - A_{(CH_3)_2COO}))$, where $A_{(CH_3)_2COO} = 5$. In both terms, $x = 5$, and has been optimized to improve the fit between
 490 measured and calculated total SCI yields of larger alkenes (Newland et al., 2020).

491 Figure 5 shows the measured CI* stabilisation for CH_2OO and $(CH_3)_2COO$ as a function of the total
 492 energy taken from the POZ by the CI*, from Newland et al. (2020). Fits to the measured data are calculated using
 493 Eq. (2). Also shown are the calculated stabilisation trends for (*E*)- and (*Z*)- CH_3CHOO and nopinone oxide (the C_9
 494 CI* formed in β -pinene ozonolysis). Figure 5 shows that stabilisation of *E*-CI* is predicted to be considerably
 495 greater than for *Z*-CI* when formed with the same energy. For CH_3CHOO it is noted that very little (0.11)
 496 stabilisation of (*Z*)- CH_3CHOO^* is predicted when produced from but-2-ene ozonolysis (fraction of total energy
 497 $= A_{CI}/A_{tot} = 4/7 = 0.57$), whereas a much greater stabilisation of (*E*)- CH_3CHOO^* is predicted. Using the *E/Z*-
 498 $RCHOO$ yields given in Section 2.8.2 for *cis* and *trans* alkenes, and the trends presented in Figure 5, then a total
 499 SCI yield of 0.33 for *trans*-but-2-ene and 0.42 for *cis*-but-2-ene is calculated, in good qualitative agreement with
 500 the relationship observed in Newland et al. (2015). The calculated values for nopinone oxide demonstrate the
 501 decreasing sensitivity of CI* stabilisation to the co-product size as the size of the CI* increases.



502
 503 **Figure 5. Dependence of CI* stabilisation on the fraction of the total energy taken from the POZ. Black (CH_2OO) and red ($(CH_3)_2COO$) points, measurements taken from Newland et al. (2020). Solid and dashed lines, fits calculated using Eq. (2).**
 505

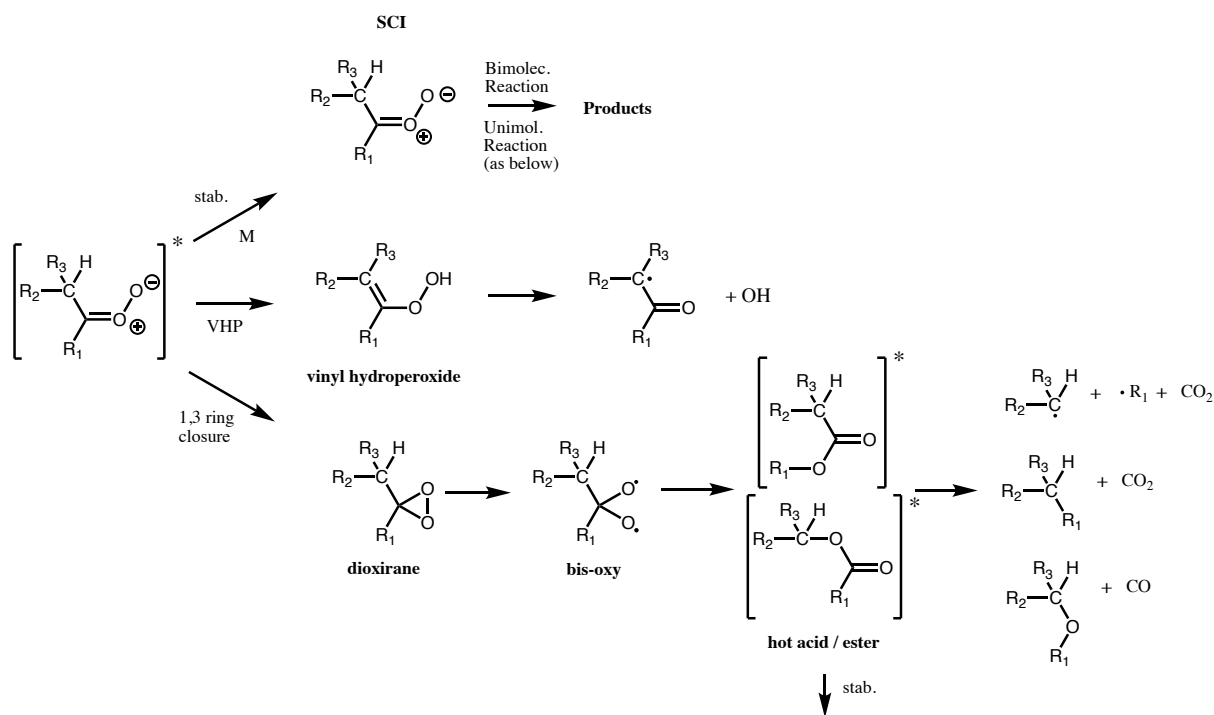
506 For endocyclic alkenes, an empirically derived sigmoid fit (Supplementary Section S2: Equation S1; Figure
 507 S6) is applied to the very limited dataset that shows $Y_{SCI} \approx 0$ for $C \leq 7$, $Y_{SCI} \approx 0.2$ for monoterpenes, and $Y_{SCI} \approx$
 508 0.74 for sesquiterpenes.

509 4 Unimolecular reactions of CI* and SCI

510 CI can undergo unimolecular isomerisation / decomposition. The unimolecular pathways available to SCI are
 511 assumed to be the same as those available to CI* (although it is noted that there is little evidence to back up this

512 assumption). However, while for CI* these processes are prompt, occurring on a timescale of 10^{-9} s (Drozd et al.,
 513 2017), for SCI they occur at a range of rates such that their competition with atmospheric bimolecular reactions
 514 needs to be considered. A wide range of unimolecular isomerisation / decomposition pathways have been
 515 characterised for CI, but only two of these are believed to be important for saturated CI under atmospheric
 516 boundary layer conditions (Vereecken et al., 2017): a 1,4 H-migration, i.e. the vinylhydroperoxide pathway, and
 517 a 1,3 ring closure, i.e. the hot acid / ester pathway (Figure 6). If the vinylhydroperoxide pathway is available, then
 518 this will always be the dominant decomposition pathway as it is the energetically most facile, with only a slight
 519 entropic disadvantage compared to the 1,3 ring closure (Vereecken et al., 2017). Unsaturated CI have some
 520 additional pathways available (see Section 4.4).

521 Experimentally determined decomposition rates are available only for a limited number of SCI. Early
 522 estimates were considerably slower than more recent experimental evidence. Vereecken et al. (2017) recently
 523 published an extensive SAR providing temperature dependent unimolecular rates and mechanisms for a wide
 524 range of SCI structures based on theoretical calculations tied to experimental work as well as group additivity
 525 relations.



526

527 **Figure 6. Available pathways for a CI with a hydrogen atom available in beta position to the carbonyl oxide. From top**
 528 **to bottom, the available pathways are the stabilisation (stab.) pathway, the vinylhydroperoxide (VHP) pathway and**
 529 **the 1,3 ring closure (hot acid/ester) pathway.**

530 4.1 Vinylhydroperoxide (VHP) pathway

531 A CI with a β -hydrogen atom in a *syn* orientation to the terminal oxygen atom of the carbonyl oxide can isomerise
 532 to form a vinylhydroperoxide via a 5-membered transition cycle (Figure 6). This route is therefore available to
 533 monosubstituted (*Z*)-CIs and disubstituted CIs. The VHP formed has a short lifetime and promptly or thermally
 534 decomposes to form an OH radical and a β -acylalkyl (vinoxy) radical, in some cases with a small yield of β -acyl-
 535 alcohols (Taatjes et al., 2016; Kuwata et al., 2018). The OH radicals are thus formed on a short time scale (e.g.
 536 Drozd et al., 2017) directly from the VHP decomposition. The β -acylalkyl radical reacts with O_2 to form a β -

537 acylperoxy radical. On a longer timescale, the subsequent chemistry of this peroxy radical can yield further HO₂
538 and OH radicals (e.g. Nguyen et al., 2016).

539 The best studied system that follows the 1,4 H-shift pathway is stabilised (CH₃)₂COO. Experimentally
540 derived rates are fast (300 – 1000 s⁻¹) (Berndt et al., 2014b; Newland et al., 2015; Chhantyal-Pun et al., 2016;
541 Smith et al., 2016). The experimental evidence also shows a strong temperature dependence, with measured rates
542 varying from 269 s⁻¹ at 283 K to 916 s⁻¹ at 323 K (Smith et al., 2016). This is in good agreement with the SAR of
543 Vereecken et al. (2017) which shows that the rate of decomposition of saturated SCI is fastest (*ca.* 500 s⁻¹) for
544 those SCI with access to the VHP route. This SAR shows that the rate is slowed by more than an order of
545 magnitude when only one H atom is available on the α-carbon and that the rates are also affected by the *anti*-
546 substituent, with the presence of a vinyl group reducing rates by an order of magnitude, and the presence of a
547 carbonyl group reducing rates by two orders of magnitude.

548 This pathway may not be available to certain CI structures even though there is an available hydrogen on
549 the α-carbon. This is the case for the bicyclic C₉ CI formed in ozonolysis of the monoterpene β-pinene, with the
550 terminal oxygen facing the four membered ring. Calculations have shown that formation of the vinyl
551 hydroperoxide is not possible for this CI due to the strain it would put on the ring, and so the dominant
552 decomposition pathway is 1,3 ring closure (Nguyen et al., 2009b). This has also been shown to be the case for the
553 cyclic C₉ CI formed facing the three membered ring in the ozonolysis of sabinene (Almatarneh et al., 2019).

554 4.2 1,3 ring closure

555 For monosubstituted (*E*)-CI and CH₂OO (see Section 5.3), decomposition via a VHP is not available. Instead
556 unimolecular reaction proceeds predominantly via a 1,3 ring closure, with typical rates ≤ 10² s⁻¹ (Vereecken et al.
557 2017), to a chemically activated dioxirane species (Figure 6). This breaks the weak O-O bond giving a singlet bis-
558 oxy radical (Wadt and Goddard, 1975; Herron and Huie, 1977; 1978). Various pathways have been proposed for
559 the subsequent chemistry of this species based on observed product distributions (Chen et al., 2002). This pathway
560 has been characterised best for CH₂OO (Section 5.3). The dioxirane is thought to rearrange to a ‘hot’ acid / ester,
561 which can undergo decomposition to yield a range of products. As the size of the CI increases, the hot acid / ester
562 is predicted to be more likely to be collisionally stabilised (Vereecken and Francisco, 2012).

563 There have been very few experimental studies to date on the products of isomerisation / decomposition
564 of (*E*)-RCHOO. This is challenging experimentally as (*E*)-RCHOO will always be formed as a partner with (*Z*-
565 RCHOO. The most studied (*E*)-CI is (*E*)-CH₃CHOO, with observed products from *cis/trans*-but-2-ene ozonolysis
566 (which yields (*E*)- and (*Z*)-CH₃CHOO as the CI products) of HCHO, CH₃COOH, CH₃OH, CH₄, CHOCHO,
567 ketene, CO and CO₂ (e.g. Tuazon et al., 1997; Grosjean et al., 1994). With the exception of glyoxal, these can all
568 be rationalised as decomposition products of ‘hot’ (*E*)-CH₃CHOO via various pathways (Reactions R1 – R5). The
569 relative proportion of each channel is based on the reported yields in Tuazon et al. (1997), except for CH₃COOH,
570 from Grosjean et al. (1994), although it is noted that CH₃COOH may be a product of CH₃CHOO + water vapour
571 in their experimental setup.



576	$\text{H}_2\text{CCO} + \text{H}_2\text{O}$	10 %	(R4)
577	CH_3COOH	20 %	(R5)

578
579 For $\text{R}_1\text{R}_2\text{COO}$ decomposition via 1,3 ring closure, products are formed via a ‘hot’ ester. There has been very little
580 work on the relative contribution of decomposition channels and stabilisation for these species. For example, there
581 is no experimental work to validate the predicted trend of increasing stabilisation of the hot acid / ester with size,
582 or at what size this becomes important. For the large terpenoid compounds β -pinene (Nguyen et al., 2009b) and
583 β -caryophyllene (Nguyen et al., 2009a), the acids/lactones formed from isomerisation of the C_9 -dioxirane have
584 been predicted to be fully stabilised.

585
586

587 4.3 CH_2OO

588 CH_2OO also follows the 1,3-ring closure pathway but is considered separately here as it has been the subject of a
589 considerable body of work. Experimentally reported products from CH_2OO decomposition include: CO_2 , CO , H_2 ,
590 OH , HO_2 , H_2O , and HCOOH (e.g. Calvert et al., 2000). Recent theoretical (Nguyen et al., 2015; Stone et al., 2018;
591 Peltola et al., 2020) works suggest that the only reaction pathway of the bis-oxy radical important under
592 tropospheric conditions is isomerisation to ‘hot’ formic acid, followed by decomposition to either $\text{H}_2 + \text{CO}_2$ or
593 $\text{H}_2\text{O} + \text{CO}$, in agreement with experimental and theoretical work on acid pyrolysis experiments (Chang et al.,
594 2007; Vichiatti et al., 2017). Due to the large excess energy and its small size, very little of the hot acid is stabilised,
595 with measured HCOOH yields from ethene ozonolysis < 5% (Calvert et al., 2000) (and the latter may be due to
596 bimolecular reactions of SCI rather than stabilisation of the hot acid). Stone et al. (2018) and Peltola et al. (2020)
597 considered the decomposition of stabilised CH_2OO using master equation simulations, determining the major
598 decomposition channel to be $\text{H}_2 + \text{CO}_2$ (64 % and 61% respectively), with the $\text{H}_2\text{O} + \text{CO}$ accounting for the
599 remainder (36%) in Stone et al. (2018), while Peltola et al. (2020) also found a small contribution (~8%) from the
600 $\text{OH} + \text{HCO}$ channel. It is noted that previous experimental work on ethene ozonolysis (Su et al., 1980; Horie et al.,
601 1991; Neeb et al., 1998) has generally inferred a preference for the $\text{H}_2\text{O} + \text{CO}$ channel. This may be due to different
602 pathways being followed by the dioxiranes formed from the excited CH_2OO produced in the ozonolysis reaction
603 compared to those formed from stabilised CH_2OO , as suggested by work on larger systems (Nguyen et al., 2009a;
604 2009b), and in the calculations of Nguyen et al. (2015) on excited CH_2OO decomposition in ethene ozonolysis. A
605 decomposition pathway to $\text{HCO} + \text{OH}$, proposed as the source of observed OH yields of 8-15 % in earlier
606 experimental studies on the ozonolysis of ethene (Gutbrod et al., 1997; Rickard et al., 1999; Kroll et al., 2001;
607 Alam et al., 2011) and larger alkenes (Kroll et al., 2002), has recently been determined experimentally to be
608 negligible (Stone et al., 2018), accounting for less than 2 % of the overall decay. This is in agreement with earlier
609 theoretical work (Olzmann et al., 1997; Nguyen et al., 2015) suggesting negligible OH yields from ethene
610 ozonolysis. This apparent discrepancy between experiment and theory can be reconciled by invoking the
611 possibility of OH formation via the carbonyl-hydroperoxide channel in the POZ decomposition, as discussed in
612 Section 2.7.

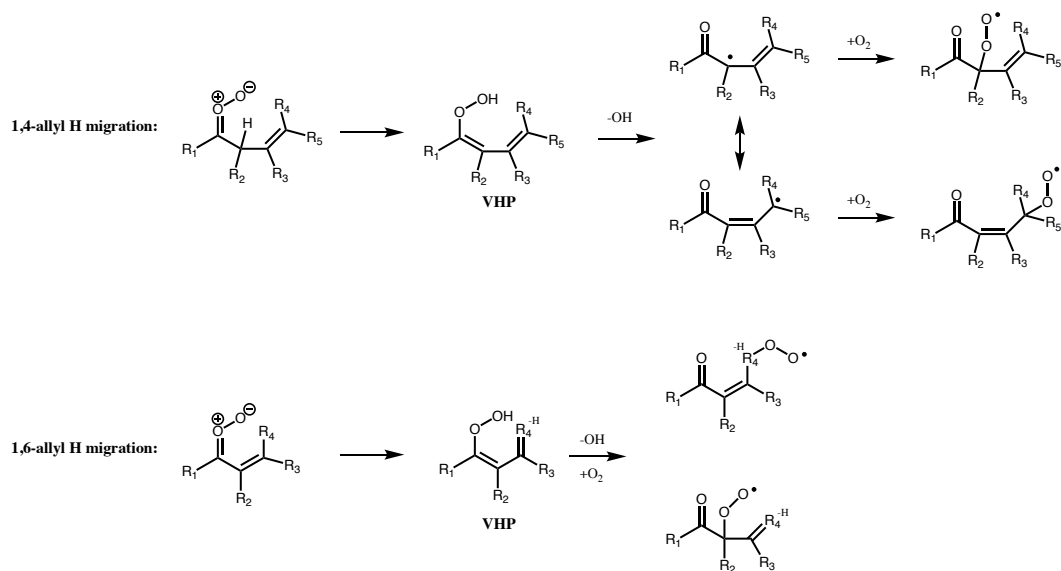
613 The unimolecular decomposition rate of stabilised CH_2OO has been experimentally determined to be very
614 slow (<12 s^{-1}) (Berndt et al., 2015; Chhantyal-Pun et al., 2015; Newland et al., 2015; Stone et al., 2018; Peltola et

615 al., 2020), with a current recommendation by IUPAC of $\leq 0.2 \text{ s}^{-1}$ at 1 bar and 298 K (Cox et al., 2020). Even at
 616 the upper end of these estimates, decomposition is a negligible atmospheric fate for stabilised CH_2OO compared
 617 to reaction with water vapour.

618 4.4 Unimolecular reactions of unsaturated CI

619 The ozonolysis of conjugated alkenes proceeds via the same initial POZ mechanism as non-conjugated systems,
 620 but decomposition of the POZ leads to the formation of unsaturated CI and/or carbonyls. While many of the
 621 characteristics of the chemistry are expected to be similar, the theoretical work of Kuwata et al., (2005), Kuwata
 622 and Valin (2008), and Vereecken et al. (2017) has shown some important differences. Specifically, additional
 623 unimolecular decomposition channels (Figure 7 and Figure 8) become available, which in some cases are faster
 624 than the 1,4 H-shift channel.

625

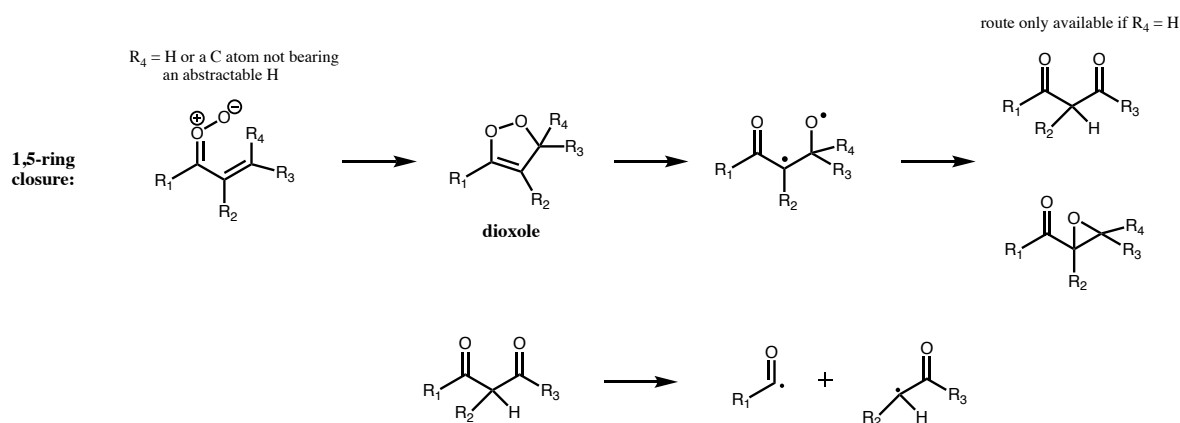


626

627 **Figure 7. Dominant unimolecular decomposition routes available to unsaturated CI with the terminal oxygen *syn* to an**
 628 **α or β vinyl group. Pathways available if terminal oxygen is *anti* to a vinyl group are the same as for saturated CI. For**
 629 **1,5-ring closure see Figure 8.**

630 If the vinyl group of an unsaturated CI is *anti* to the terminal oxygen of the carbonyl oxide, then the molecule will
 631 follow one of the two routes available to saturated CI, but with a rate affected by the presence of the double bond.
 632 However, if the vinyl group is *syn* to the terminal oxygen, alternative mechanisms of decomposition are available.
 633 1,4 and 1,6-allyl H-migration (for the vinyl group being in β or α position respectively), are available if an H atom
 634 is present on the α or γ carbon. These pathways lead to similar products to 1,4-alkyl H-migration, with a
 635 vinylhydroperoxide intermediate decomposing to give OH and one of two possible unsaturated peroxy radicals.
 636 If no H-atom is available for (*Z*)- β -unsaturated CI then they follow the 1,3-ring closure channel with SCI
 637 decomposition rates $\leq 1 \text{ s}^{-1}$. The rates of the 1,6-allyl H-migration channel for SCI are of the order of 10^6 s^{-1} , while
 638 1,4-allyl H-migration of SCI has rates ranging from $10^1 - 10^4 \text{ s}^{-1}$ depending on other substituents (Vereecken et
 639 al. 2017).

640 For CI with the carbonyl oxide *syn* to an α vinyl group, and without an available hydrogen on the α
 641 carbon, then the dominant decomposition mechanism is 1,5 ring closure, originally proposed by Kuwata et al.
 642 (2005) (Figure 8). This forms an intermediate dioxole species with a five membered ring. This is predicted to have
 643 high internal energy and to break the O-O bond, leading to an epoxy carbonyl, or, if $R_4 = H$, to a dicarbonyl
 644 (Kuwata 2005). The dicarbonyl has been predicted to undergo further prompt decomposition via various possible
 645 unimolecular channels, some of which appear to yield OH (Barber et al., 2018). Based on the stable product
 646 distribution from *anti*-MVKO decay, the decomposition of the dicarbonyl has been determined to be
 647 predominantly via C-C cleavage leading to two radicals (acetyl and vinoxy radicals in the case of *anti*-MVKO)
 648 (Vansco et al., 2020). These radicals will add O_2 leading to RO_2 radicals which may undergo further
 649 decomposition if formed chemically excited, ultimately to $HCHO + OH + CO$ in both cases (Carr et al., 2011;
 650 Weidman et al., 2018; Vansco et al., 2020). For *syn*-MACRO, Vansco et al. (2020) determine a pathway via a
 651 dioxole analogous to that just described, leading to formyl and 2-methyl vinoxy radicals, the latter of which could
 652 ultimately yield $CH_3CHO + OH + CO$. However, this accounts for only about half of the decomposition of the
 653 dicarbonyl, with the other half leading to acrolein via an unidentified unimolecular process. It is noted that Barber
 654 et al. (2018) and Vansco et al. (2020) did not consider the epoxide isomerisation pathway for the dioxole. The
 655 calculated unimolecular decay rates for the dioxole forming pathways from *syn*-MACRO and *anti*-MVKO are
 656 fast; Vereecken et al. (2017, Table 25 in supplementary material) reported rates of 2500 and 7700 s^{-1} , respectively,
 657 with increasing substitution on the vinyl group accelerating the reaction further, while Barber et al. (2018) reported
 658 a somewhat slower rate for *anti*-MVKO of 2140 s^{-1} . Decay of stabilized *syn*-MVKO is relatively slow at 33 – 50
 659 s^{-1} (Vereecken et al., 2017; Barber et al., 2018) making it a potentially important bimolecular reaction partner in
 660 the atmosphere.
 661



662
 663 **Figure 8. 1,5-ring closure: dominant unimolecular pathway for unsaturated CI with the terminal oxygen *syn* to an α**
 664 **vinyl group and R_4 is not a carbon with an abstractable hydrogen.**

665 4.5 Protocol Rules for CI decomposition

666 For unimolecular decomposition of CI, the SAR of Vereecken et al. (2017) is used to determine decomposition
 667 pathways and rates (for SCI). The products from each decomposition pathway are given in Table 2, where any
 668 secondary reactions such as recombination with O_2 are already accounted for. The vinylhydroperoxide pathway
 669 is assumed to lead exclusively to a β -oxo alkyl radical and OH. For decomposition via 1,3 ring closure, the hot
 670 acid / ester formed is considered to decompose via one of the three major pathways determined for (*E*)-RCHOO:

671 RH + CO₂ (40%), ROH + CO (20%), R + HO₂ + CO₂ (40%), based on the observed product yields from *cis* and
 672 *trans* but-2-ene experiments by Tuazon et al. (1997). While it is noted that Grosjean et al. (1994) observed a
 673 CH₃COOH yield of ~ 20 %, this could also be a product of CH₃CHOO + water vapour in their experimental setup.
 674 For larger CI (≥C₉) the acid / ester is considered to be fully stabilised, if two esters can be formed they are
 675 considered equally likely. This is recognised as an area where detailed experimental studies are required, to
 676 establish the sensitivity of acid / ester stabilisation to CI size, as well as identifying decomposition products for a
 677 range of CI sizes / structures, and whether these are different for chemically activated / thermalized dioxiranes, as
 678 predicted (Anglada et al., 1998; Nguyen et al., 2009a, 2009b). For CH₂OO decomposition, the protocol assigns
 679 the products equally to two decomposition pathways: H₂+CO₂ and H₂O+CO; as discussed above, no OH is formed
 680 directly.

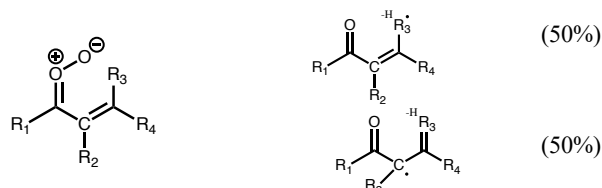
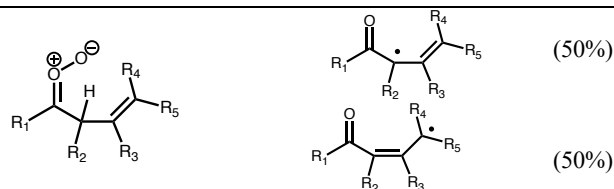
681 For 1,4-and 1,6 allyl H-migration in unsaturated CI (Figure 7), formation of the alkyl radicals from each
 682 of the delocalized radical sites formed after OH elimination is assumed to be equally likely. The product yields
 683 given in Table 2 are for mechanisms that do not explicitly preserve stereo-specificity. For systems that track
 684 stereo-specific substitution on double bonds, H-migration is only possible from the *Z*-substituent, and the number
 685 of products is reduced accordingly, with a concomitant adjustment of the product yields.

686 For 1,5 ring closure (Figure 8), formation of the epoxide or the dicarbonyl are considered equally likely.
 687 The dicarbonyl undergoes further decomposition to yield two RO₂ following Barber et al. (2018). Unimolecular
 688 reaction rates for stabilised unsaturated CI are taken from the Vereecken et al. (2017) SAR. Clearly there remains
 689 much uncertainty on the proposed kinetics, and systematic experimental work on SCI yields, and final product
 690 studies of ozonolysis of conjugated alkenes is required to improve the proposed protocol.

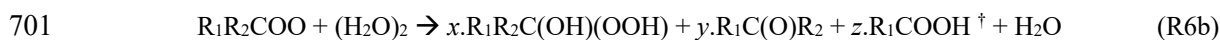
691

692 **Table 2. Decomposition pathways and products for CI in the protocol**

Decomposition Pathway	CI Structure	Products
1,4 H-shift (VHP)		
1,3 ring closure (hot acid / ester) CI < C₉		R ₁ R ₂ + CO ₂ (40 %) R ₁ OR ₂ + CO (20 %) R ₁ + R ₂ + CO ₂ (40 %)
1,3 ring closure (hot acid / ester) CI ≥ C₉		R ₁ CO-O-R ₂ (50%) R ₁ -O-COR ₂ (50%)
CH₂OO		H ₂ +CO ₂ (50 %) H ₂ O+CO (50 %)
1,5-ring closure	R ₄ = H or a C atom not bearing an abstractable H 	
1,5-ring closure (R₃ = H)	R ₄ = H or a C atom not bearing an abstractable H 	(50%) R ₁ C(O)O ₂ + CHOC(O ₂)R ₂ (50%)

1,6 allyl H-shift**1,4 allyl H-shift****693 5 Bimolecular Reactions of SCI**

694 Based on the unimolecular pathways described in Section 5, many SCI have lifetimes against unimolecular
695 reaction on the order of $10^{-3} - 10^{-1}$ s. These lifetimes are long enough to allow them to participate in bimolecular
696 reactions with trace gases in the atmosphere under typical boundary layer conditions, where Vereecken et al.
697 (2017) estimated that just under half of the CI in the atmosphere react with a co-reactant rather than
698 unimolecularly. The co-reactants for which fast reactions, of potential tropospheric importance, have been
699 demonstrated are H_2O , $(\text{H}_2\text{O})_2$, SO_2 , NO_2 , and organic and inorganic acids (Reactions 6 – 11).



702 † only available if $\text{R}_2 = \text{H}$



708 Reactions with other trace gases have been investigated both experimentally and theoretically, but these are not
709 included in the protocol at this time as they are not considered to be important under tropospheric conditions.
710 Theoretical and experimental work has also shown that more complex bimolecular and unimolecular pathways
711 may operate forming heterocyclic molecules like cyclic peroxides and secondary ozonides (Chuong et al., 2004;
712 Long et al., 2019). Again though, these reactions appear to be of negligible importance in the gas phase for SCI
713 with carbon numbers up to C_{10} (monoterpenes) and are not considered in this protocol. While only reactions
714 relevant to the atmosphere are included in the protocol; reactions that are not expected to be relevant in the
715 atmosphere are still maintained in the database since they may be useful to interpret results of chamber simulations
716 or other laboratory experiments (e.g. self-reaction or reaction with parent alkenes).

717 CH_2OO and (*E*)- RCHO react rapidly with H_2O (Reaction R6a) (Welz et al., 2012; Taatjes et al., 2013;
718 Stone et al., 2014) and with the water dimer, $(\text{H}_2\text{O})_2$, (Reaction R6b) (Berndt et al., 2014a; Chao et al., 2015;
719 Lewis et al., 2015; Lin et al., 2016), such that removal by water vapour is their predominant fate in the atmosphere.
720 However, (*Z*)- RCHO react slowly with H_2O (Taatjes et al., 2013; Sheps et al., 2014; Huang et al., 2015)
721 increasing the importance of bimolecular reactions with other atmospheric trace species such as acids and SO_2

722 (Newland et al., 2018). The reaction of SCI with organic acids (Reaction R7) is also likely to be an important
723 reaction in the atmosphere (Welz et al., 2014). The experimentally determined reaction rates for SCI + HCOOH
724 and CH₃COOH are $1 - 5 \times 10^{-10} \text{ cm}^3 \text{ s}^{-1}$ (Welz et al., 2014; Sipilä et al., 2014; Chung et al., 2019), close to the
725 collisional limit. Other potentially important reactions in the atmosphere include those with SO₂ (Reaction R8),
726 NO₂ (Reaction R9), and inorganic acids (Reactions R10-R11). The rates of SCI+SO₂ reaction have been the
727 subject of several studies for the three smallest SCI, with good agreement between experiments. Larger SCI appear
728 to have similar reaction rates with SO₂ (Ahrens et al., 2014).

729 The products of many of the bimolecular reactions of SCI are still uncertain. This is the case for the most
730 important bimolecular reactions in the atmosphere, those with H₂O and (H₂O)₂. A recent experimental study
731 (Sheps et al., 2017) of the reaction of CH₂OO with the (H₂O)₂, generating CH₂OO from the photolysis of
732 diiodomethane, determined yields of: hydroxymethylhydroperoxide (HMHP) (55 %), HCHO (40 %), and
733 HCOOH (5 %). However, ozonolysis experiments (e.g. Nguyen et al., 2016) have generally found HMHP and
734 HCOOH to be the main detected products, with negligible yields of HCHO. Based on results from isoprene
735 ozonolysis chamber experiments, Nguyen et al. (2016) proposed yields from the CH₂OO + H₂O reaction of:
736 HMHP (73 %), HCOOH (21 %), HCHO (6 %); and from the (H₂O)₂ reaction of: HMHP (40 %), HCOOH (54 %),
737 HCHO (6 %). These low HCHO yields are in agreement with earlier work (Hasson et al., 2001b) that determined
738 an HCHO yield of 6 – 9 %.

739 The products of SCI reaction with organic acids appear to be mainly hydroperoxide esters (Reaction R7).
740 Hydroperoxy methyl formate (HPMF) has been detected as an intermediate in the CH₂OO+HCOOH reaction (e.g.
741 Neeb et al., 1995; Wolff et al., 1997; Hasson et al., 2001a; Chung et al., 2019), hydroperoxy methyl acetate in the
742 CH₂OO+CH₃COOH reaction (Neeb et al., 1996), and hydroperoxy ethyl formate in the CH₃CHOO+HCOOH
743 reaction (Neeb et al., 1995; 1996; Cabezas and Endo, 2020). Theoretical calculations have predicted the formation
744 of > 90 % HPMF for the reaction of CH₂OO with HCOOH (Vereecken, 2017), and that the production of stabilised
745 hydroperoxide esters will be even higher for larger SCI. The reaction with SO₂ has been shown to form SO₃ with
746 close to unit yield (Reaction R8) (Kuwata et al., 2015). For NO₂, while early experimental work (Ouyang et al.,
747 2013) suggested SCI would oxidise NO₂ to NO₃, more recent experimental (Caravan et al., 2017) and theoretical
748 (Vereecken and Nguyen, 2017) work has suggested the formation of a nitroalkylperoxy radical (R₁R₂C(O₂)NO₂).
749 Subsequent reaction and formation of the alkoxy radical would be expected to yield a carbonyl and NO₂. The
750 main products of reaction of SCI with the inorganic acid HCl have been predicted to be chlorohydroperoxides
751 (Reaction R10) (Foreman et al., 2016; Vereecken, 2017), with these products observed experimentally for
752 CH₂OO+HCl (Cabezas and Endo, 2017; Taatjes et al., 2021) and CH₃CHOO+HCl (Cabezas and Endo, 2018).
753 The main product of reaction with HNO₃ has been predicted to be hydroperoxynitrates (Reaction R11) (Foreman
754 et al., 2016; Raghunath et al., 2017; Vereecken, 2017). Raghunath et al. (2017) further predicted decomposition
755 of a fraction of the chemically activated hydroperoxynitrates to CH₂(O)NO₃ + OH. This reaction has not yet been
756 studied experimentally to the authors' knowledge.

757 5.1 Protocol Rules for SCI Bimolecular Reactions

758 Bimolecular reaction rate coefficients for SCI are included for reaction with water vapour monomers and dimers,
759 SO₂, NO₂, carboxylic acids and inorganic acids (HCl, HNO₃) (Table 3). For the water vapour reactions, the rate
760 coefficients are taken from the SAR of Vereecken et al. (2017), which provides values for 98 explicit structures.

761 For bimolecular reactions of SCI with the other trace gases, four classes of SCI are considered: CH₂OO, *Z/E*-
 762 RCHOO and R₁R₂COO (where R represents alkyl groups), based on the limited experimental data available. The
 763 rates are taken from IUPAC recommendations (Cox et al., 2020) where available, otherwise from sources as stated
 764 in Table 3. Where the structure does not fit into the defined classes, the CH₂OO rate constant is attributed by
 765 default. Reaction products are as given in Reactions R6 – R11. In light of the current uncertainties of the product
 766 distribution of the reactions of SCI with water, here we assume the same products for the monomer and dimer
 767 reactions. We propose yields based on the direct study of Sheps et al. (2017) of α -hydroxyhydroperoxide (55 %),
 768 carbonyl (40 %) and acid (5 %), with the exception of R₁R₂COO, which cannot form the acid, for which we
 769 increase the α -hydroxyhydroperoxide to 60 %. These recommendations will be subject to change upon further
 770 experimental information becoming available.

771 **Table 3. Bimolecular reaction rates with RCOOH, SO₂, NO₂ and inorganic acids applied to the four SCI structures.**
 772 **Rates are IUPAC recommendations (Cox et al., 2020) unless otherwise stated. Bimolecular reaction rates with water**
 773 **are taken from Vereecken et al. (2017), see main text.**

	Bimolecular reaction rates (10 ¹¹ cm ³ molecules ⁻¹ s ⁻¹)				
	RC(O)OH	SO ₂	NO ₂	HCl ^a	HNO ₃ ^a
CH ₂ OO	12	3.7	0.3	4.6	54
(<i>E</i>)-RCHOO ^b	38 ^c	14	0.2	4.6	54
(<i>Z</i>)-RCHOO ^b	21 ^c	2.6	0.2	4.6	54
R ₁ R ₂ COO	31	16	0.2	4.6	54

774 ^a All values for CH₂OO reaction from Foreman et al. (2016); ^b IUPAC recommended values for (*E*) and (*Z*)-CH₃CHOO; ^c
 775 Mean of IUPAC recommended values for reaction with HCOOH and CH₃COOH.
 776

777 6 Example of protocol application

778 An example is described below for the unsaturated ketone, 6-methyl-5-hepten-2-one, and illustrated in Figures 9
 779 and 10. Further examples for α -pinene, *cis*-2-pentene, 2-methyl-1-pentene and 2-methyl-1,3-butadiene (isoprene)
 780 are given in the Supplementary (Section S3). The initial rate of reaction with ozone is defined by the protocol in
 781 the companion paper (Jenkin et al., 2020). The branching ratio for formation of the disubstituted CI* is calculated
 782 to be 0.72 using the group additivity values in Table 2 and Eq. (1).
 783

$$784 \quad Y_{\text{CI1}} = \frac{(0.218+0.218)-(0+0)+1}{2} = 0.72 = 1 - Y_{\text{CI2}} \quad (\text{E3})$$

785
 786 The *syn* and *anti*-conformers of the two large CI* are formed with equal yield (0.14).

787 Stabilisation of each CI* is computed using Eq. (2):

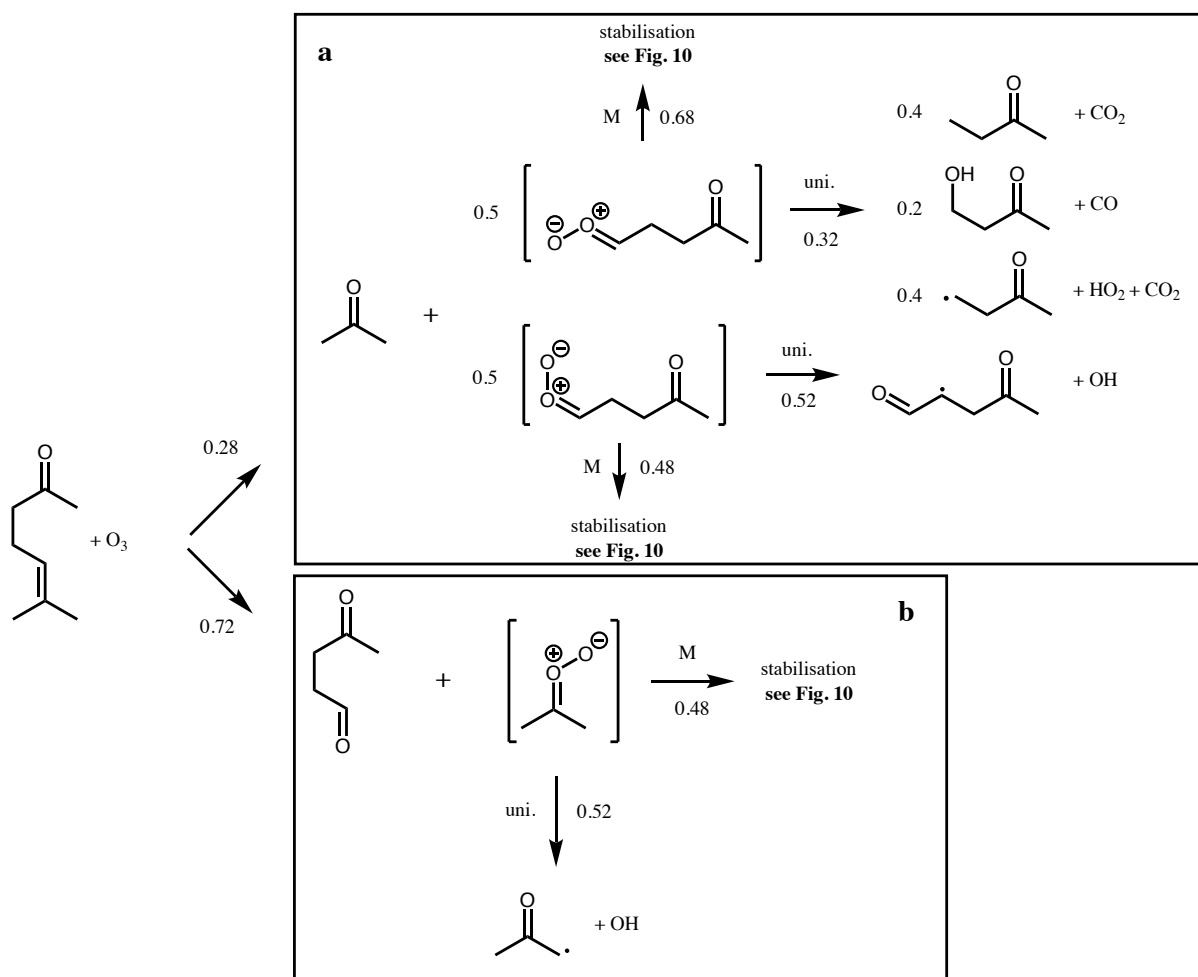
$$788 \quad (\text{CH}_3)_2\text{COO}: \quad S = 1 - \left[\left(\frac{5}{12} \right) \times 1.242 \times \left(\frac{5}{5+(5-5)} \right) \right] = 0.48 \quad (\text{E4})$$

$$790 \quad (\text{Z})\text{-CH}_3\text{C(O)}(\text{CH}_2)_2\text{CHOO}: \quad S = 1 - \left[\left(\frac{8}{12} \right) \times 1.242 \times \left(\frac{5}{8+(5-5)} \right) \right] = 0.48 \quad (\text{E5})$$

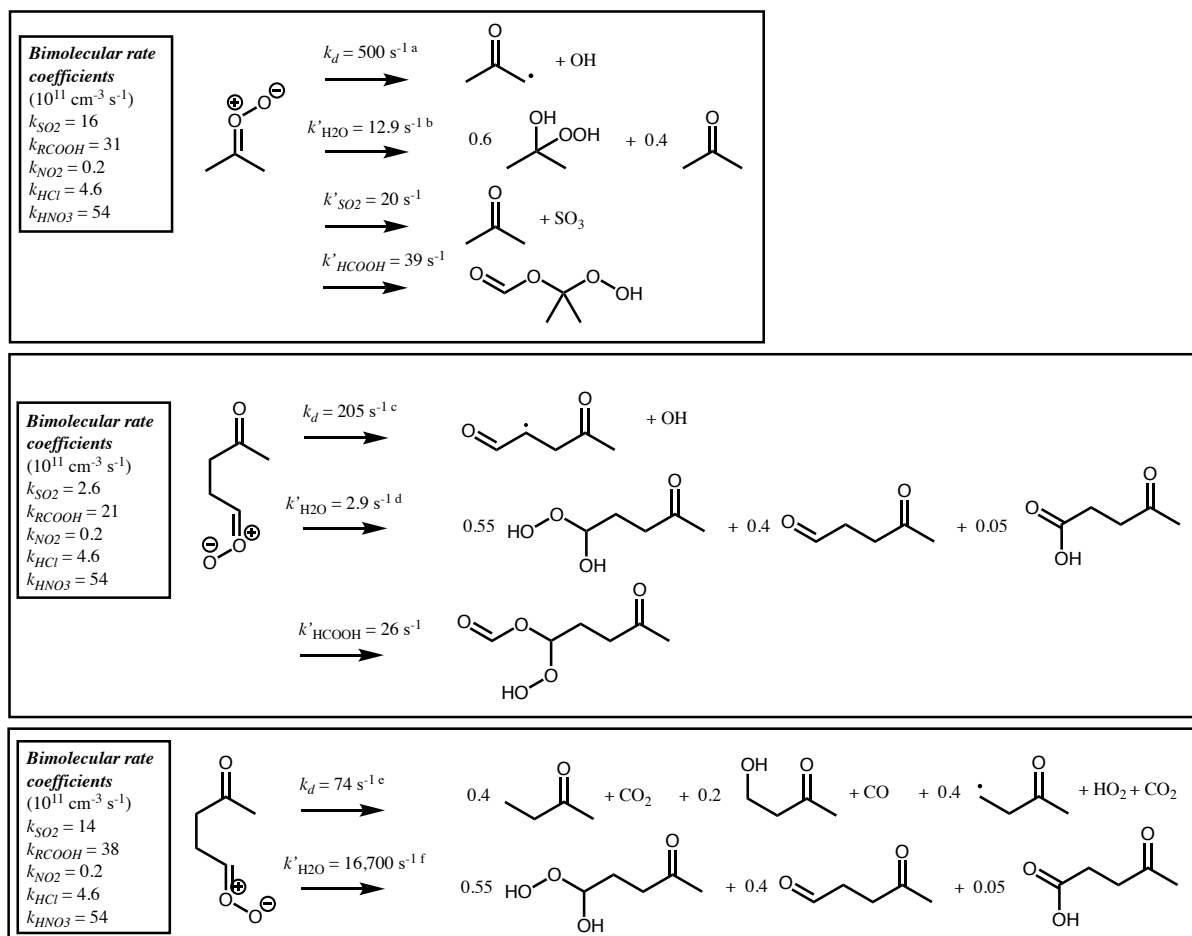
$$791 \quad (\text{E})\text{-CH}_3\text{C(O)}(\text{CH}_2)_2\text{CHOO}: \quad S = 1 - \left[\left(\frac{8}{12} \right) \times 0.95 \times \left(\frac{5}{8+(5-3)} \right) \right] = 0.68 \quad (\text{E6})$$

792
 793 The remaining (CH₃)₂COO* undergoes unimolecular decomposition via the vinylhydroperoxide (VHP) pathway
 794 to yield the acetyl peroxy radical (CH₃C(O)CH₂OO) and OH. The remaining (*Z*)-CH₃C(O)(CH₂)₂CHOO

795 decomposes via the VHP pathway to yield $\text{CH}_3\text{C}(\text{O})\text{CH}_2\text{CH}(\text{O}_2)\text{CHO} + \text{OH}$, while (*E*)- $\text{CH}_3\text{C}(\text{O})(\text{CH}_2)_2\text{CHOO}$
 796 decomposes via 1,3 ring closure and yields $\text{CH}_3\text{C}(\text{O})\text{CH}_2\text{CH}_3 + \text{CO}_2$ (40%), $\text{CH}_3\text{C}(\text{O})\text{CH}_2\text{CH}_2\text{OH} + \text{CO}$ (20%),
 797 $\text{CH}_3\text{C}(\text{O})\text{CH}_2\text{CH}_2 + \text{H} + \text{CO}_2$ (40%). Each stabilised CI can decompose via the same pathways as its respective
 798 CI*, with temperature dependent rates determined from Vereecken et al. (2017). At 298K these are 478 s^{-1} , 205 s^{-1}
 799 1 and 74 s^{-1} for $(\text{CH}_3)_2\text{COO}$, (*Z*)- $\text{CH}_3\text{C}(\text{O})(\text{CH}_2)_2\text{CHOO}$ and (*E*)- $\text{CH}_3\text{C}(\text{O})(\text{CH}_2)_2\text{CHOO}$ respectively.
 800 Alternatively, they can undergo bimolecular reaction. Reaction rates with H_2O and $(\text{H}_2\text{O})_2$ are calculated using
 801 monomer and dimer reaction rates from Vereecken et al. (2017). Reaction rates with other trace gases are taken
 802 from Table 3 for the relevant CI structure. Figure 10 shows calculated pseudo first order reaction rates for reaction
 803 with SO_2 and RCOOH assuming atmospheric mixing ratios of $[\text{SO}_2] = 5 \text{ ppbv}$ and $[\text{RCOOH}] = 5 \text{ ppbv}$.
 804



805
 806 **Figure 9. Branching ratios and products of the CI decomposition produced following ozonolysis of 6-methyl-5-hepten-**
 807 **2-one**



809
810 **Figure 10.** Bimolecular rate coefficients (see Table 3) and products of the SCI produced following ozonolysis of 6-
811 methyl-5-hepten-2-one at 298 K. Pseudo first order loss rates (k') and products are shown for decomposition and
812 reaction with water vapour, and for other pathways that contribute more than 1% of the total loss assuming $[\text{SO}_2] = 5$
813 ppbv, $[\text{RCOOH}] = 5$ ppbv, $[\text{H}_2\text{O}] = 5 \times 10^{17} \text{ cm}^{-3}$, $[(\text{H}_2\text{O})_2] = 5 \times 10^{14} \text{ cm}^{-3}$, $[\text{NO}_2] = 1$ ppbv, $[\text{HCl}] = 100$ pptv, $[\text{HNO}_3] =$
814 **100 pptv.**

815 ^a $7.64 \times 10^{-60} \times T^{23.59} e^{(2367/T)}$

816 ^b Sum of first order loss rates to water monomer ($7.54 \times 10^{-18} * [\text{H}_2\text{O}]$) and dimer ($1.82 \times 10^{-14} * [(\text{H}_2\text{O})_2]$)

817 ^c $2.41 \times 10^{-62} \times T^{24.33} e^{(2571/T)}$

818 ^d Sum of first order loss rates to water monomer ($1.51 \times 10^{-18} * [\text{H}_2\text{O}]$) and dimer ($4.31 \times 10^{-15} * [(\text{H}_2\text{O})_2]$)

819 ^e $1.57 \times 10^{10} \times T^{1.03} e^{(-7464/T)}$

820 ^f Sum of first order loss rates to water monomer ($1.58 \times 10^{-14} * [\text{H}_2\text{O}]$) and dimer ($1.75 \times 10^{-11} * [(\text{H}_2\text{O})_2]$)

821 7 Protocol Evaluation

822 7.1 Experimental databases and assessment approach

823 A database of experimentally determined carbonyl yields, OH yields and SCI yields has been assembled to
824 evaluate the new protocol (Supplement – Spreadsheets S1-S3). Experimental conditions are also recorded in the
825 database to enable some assessment of the validity of the assumptions inherent in the experimental setup.

826 The Root Mean Squared Error (RMSE) and the Mean Bias Error (MBE) were examined to assess the
827 reliability of the protocol. The RMSE and MBE are here defined as:

828

829
$$RMSE = \sqrt{\frac{1}{n} \sum_{i=1}^n (Y_{\text{protocol}} - Y_{\text{database}})^2} \quad (\text{E7})$$

$$MBE = \frac{1}{n} \sum_{i=1}^n (Y_{protocol} - Y_{database}) \quad (E8)$$

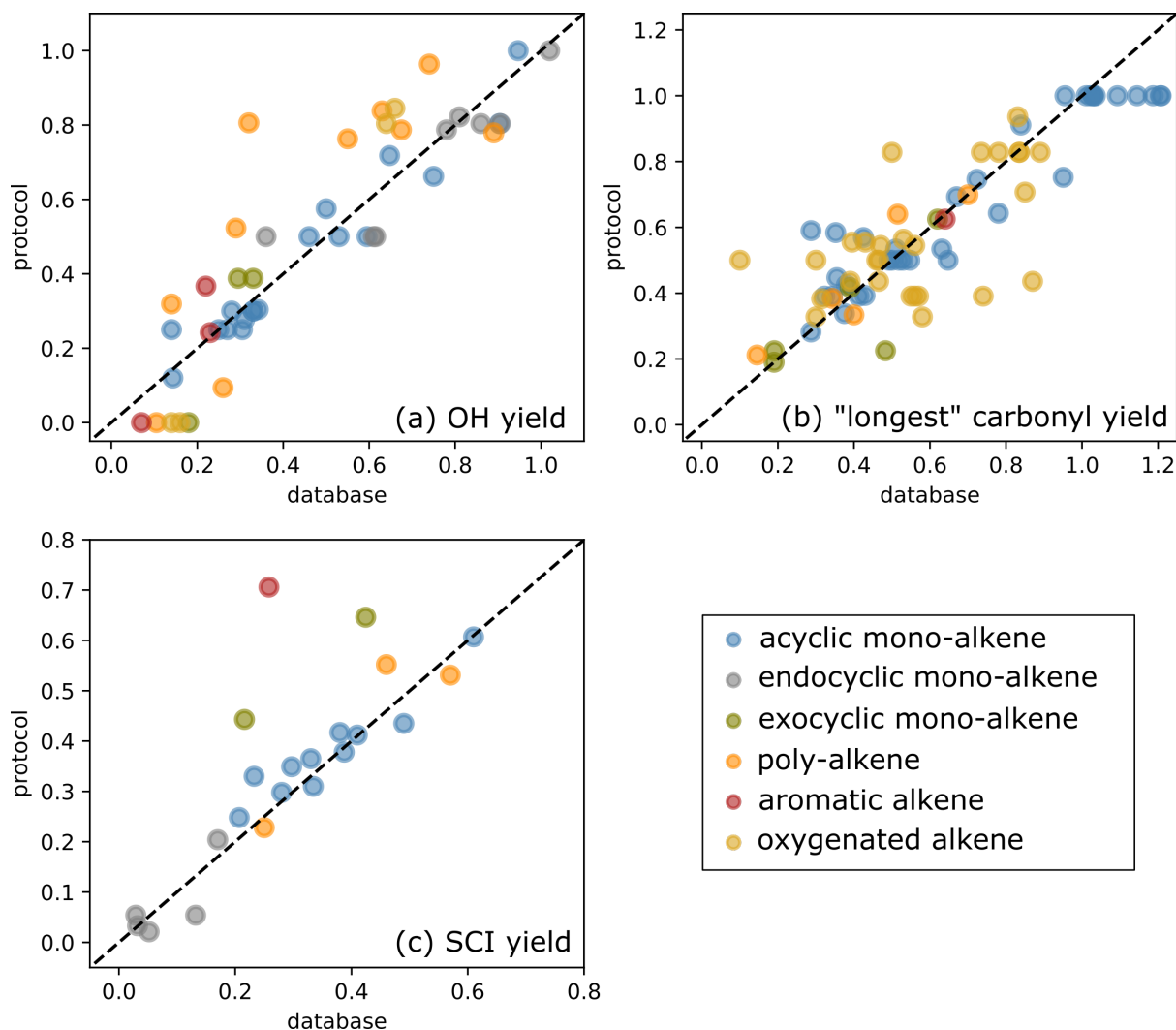
831 where n is the number of species in the dataset. The databases were split into subsets to identify possible bias
 832 within a structural category of species (e.g. exocyclic vs endocyclic monoalkenes). The various subsets examined
 833 and their corresponding number of species are summarized in Table 4. Three databases were used to perform the
 834 protocol assessment: carbonyl yields (Spreadsheet S1), SCI yield (S2), and OH yield (S3). The RMSE and MBE
 835 computed for the full databases and the various subsets are reported in Table 4. The scatter plots of protocol yields
 836 vs database yields, by species category, are given in Figure 11.

837

838 **Table 4. Number of species (n) in the database used to compute the mean bias error (MBE) and the root mean square**
 839 **error (RMSE) for the OH yields, SCI yields and "longest" carbonyl yield.**

	all species	acyclic monoalkene	endocyclic monoalkene	exocyclic monoalkene	poly alkene	aromatic alkene	oxygenated alkene
<i>OH yields</i>							
<i>n</i>	46	18	8	3	10	3	4
MBE	0.02	-0.01	-0.03	-0.01	0.13	0.03	0.01
RMSE	0.13	0.06	0.09	0.12	0.23	0.09	0.16
<i>SCI yields</i>							
<i>n</i>	22	11	5	2	3	1	0
MBE	0.05	0.02	-0.01	0.22	0.01	0.45	-
RMSE	0.12	0.04	0.04	0.22	0.06	0.45	-
<i>Yields of the longest carbonyl</i>							
<i>n</i>	73	35	NA [‡]	5	5	1	27
MBE	-0.01	-0.02	-	-0.04	0.03	-0.02	0.00
RMSE	0.14	0.11	-	0.12	0.07	0.02	0.18

840 [‡] Endocyclic alkenes do not produce a stable primary carbonyl as all possible molecules formed from the POZ fragmentation
 841 contain a carbonyl oxide moiety.
 842
 843



844
 845 **Figure 11. Scatter plot of protocol yields vs database yields: (a) OH yields, (b) yields for the "longest" carbonyl and (c)**
 846 **SCI yields.**

847 7.2 Primary Carbonyl Yields

848 The primary carbonyl yields from alkene ozonolysis are calculated in the protocol by assigning F values to
 849 different functional groups adjacent to the $C=C$ bond that determine the relative fragmentation pattern of the POZ
 850 (Section 2). The calculated primary carbonyl yields can be compared to the measurements in the experimental
 851 database. For some functional groups however, the number of data available is sparse and the carbonyl yields
 852 have been directly used to determine the F value. The carbonyl yields dataset should therefore rather be viewed
 853 as a training dataset than a validation dataset in this protocol assessment. Figure 11b shows the scatter plots for
 854 the calculated yields of the larger primary carbonyl (i.e. greater number of non-H atoms) formed in POZ
 855 decomposition, compared to the experimentally reported values for each alkene in the database. No substantial
 856 bias is identified in the computed carbonyl yields (MBE=-0.01). For non-oxygenated alkenes, the fit is reasonably
 857 good and the RMSE does not exceed 0.12 for the various hydrocarbon classes reported in Table 4. The major
 858 outlier is the yield of 4-ethyl-3-hexanone from 3,4-diethyl-2-hexene ozonolysis. This is based on one measurement
 859 (Grosjean and Grosjean, 1996a). It was noted in Jenkin et al. (2020) that the ozonolysis reaction rate reported by
 860 Grosjean and Grosjean (1996b) for this precursor compound is also a significant outlier from predicted trends.
 861 For symmetrical alkenes, the calculated primary carbonyl yield is unity, whereas measured yields tend to cluster

862 slightly above one. This is likely due to a small amount of secondary formation of the carbonyls from bimolecular
863 reactions of SCI. The poorest fitted class is oxygenated alkenes (RMSE=0.18). This is likely due to a combination
864 of factors. Firstly, the majority of these compounds have only one measurement. Secondly, measurements of
865 multi-oxygenated VOCs are known to be more challenging than e.g. simple carbonyls. Thirdly, there is more
866 likely to be additional chemical factors which are not yet understood in the ozonolysis of these more complex
867 molecules influencing the POZ fragmentation. Two of the most significant outliers in the oxygenated alkenes are
868 acrylic and methacrylic acid. As described in Section 2.2.3 it is difficult to reconcile the two available data points.

869 7.3 SCI yields

870 The yield of stabilised Criegee intermediates from an alkene-ozone reaction depends on the alkene structure (i.e.
871 the POZ fragmentation pattern, Section 2), the dominant unimolecular decomposition route of the CI* (Section
872 3.2), and the size of the CI (Section 3.2). The yields calculated by the protocol are independent of the
873 measurements in the database. SCI yields can therefore be considered as a validation dataset to evaluate the
874 reliability of the protocol. Total SCI yields have been measured for a number of alkenes, although the dataset is
875 still relatively small. It should also be noted that many experimentally determined SCI yields have a large
876 uncertainty associated with them, particularly earlier experiments where analysis techniques were less developed
877 and the chemical models lacking. Figure 11c shows the scatter plot of the total SCI yields calculated by the
878 protocol vs experimental data. The data consists predominantly of acyclic monoalkenes, for which there is a good
879 agreement between the measurements and the calculated values (RMSE=0.04). Figure 11c shows three major
880 outliers for which the protocol over-predicts the measured SCI yield. These species are methylene cyclohexane
881 and β -pinene (which constitute the subset of the exocyclic alkenes (RMSE=0.22)) and styrene, the only
882 representative of the aromatic alkenes class in this dataset (RMSE=0.45). The methylene cyclohexane and styrene
883 values are both based on one measurement (Hatakeyama et al., 1984), and the β -pinene value is based on two
884 measurements (Hatakeyama et al., 1984; Newland et al., 2018) which are in poor agreement, giving values of 0.25
885 and 0.60 respectively. This clearly warrants revisiting experimentally, particularly with respect to the
886 atmospherically important monoterpene β -pinene. Finally, the overall protocol SCI yields appear to be biased
887 slightly high (+ 5%), which is mainly explained by the overestimation described above for the exocyclic and
888 aromatic alkenes.

889 7.4 OH yields

890 The reaction of alkenes with ozone yields OH through both primary (i.e. decomposition of CI via a
891 vinylhydroperoxide) and secondary (i.e. peroxy radical chemistry) processes. The primary process can also be
892 split: the decomposition of chemically activated CI*, which under atmospheric conditions (and e.g. chamber
893 laboratory experiment conditions) is assumed to happen at rates such that there is no competition with bimolecular
894 reaction; and the decomposition of stabilised CI, which occurs in competition with bimolecular reactions so that
895 the OH yield depends on the unimolecular rate relative to the concentrations of possible co-reactants. The primary
896 OH yield thus depends on the POZ fragmentation pattern (Section 2) and the decomposition pathways of the CI
897 (Section 3.2).

898 Many studies have measured the OH yield for specific alkene-ozone reactions. As for the SCI yields
899 above, the OH yield database can be viewed as a validation dataset to assess the reliability of the protocol since

900 OH yields are not prescribed explicitly, but are a product of the protocol rules for POZ fragmentation and CI
901 decomposition pathways. For the comparison, protocol yields are computed assuming that all SCI produced
902 undergo unimolecular decomposition (i.e. bimolecular reactions of SCI are ignored). Although many experiments
903 will have been designed in such a way as to try to prevent bimolecular reactions, in reality a small fraction of the
904 SCI will react bimolecularly, not producing OH, so the computed OH yield might be considered an upper limit.
905 On the other hand, in many of the experiments there will likely be some contribution to the measured OH yield
906 from peroxy radical chemistry (e.g. $\text{HO}_2 + \text{O}_3$), making the reported experimental yield an upper limit. No attempt
907 is made here to determine the relative contribution from primary or secondary processes in the reported
908 measurements, which is dependent on both experimental setup and the particular alkene being studied, or to
909 correct for possible bimolecular reactions. Therefore, a comparison between experimental and protocol OH yields
910 clearly carries significant uncertainties.

911 With this in mind, the agreement between computed OH yields and the experimental values is very good
912 (Figure 11a). No substantial bias is observed on the complete dataset (MBE=0.02). It is difficult to comment on
913 some classes as they contain only one or two compounds (see Table 4). The protocol appears especially reliable
914 for estimating the OH yields for monoalkenes (RMSE=0.06) and endocyclic alkenes (RMSE=0.09). The class for
915 which the protocol does worst is polyalkenes (RMSE=0.23), with a systematic over-prediction at higher OH yields
916 (MBE=0.13). There are five compounds for which the protocol calculates an OH yield of zero (styrene, 1,3-
917 butadiene, methyl vinyl ketone, methacrolein, and camphene). The measured OH yields of these compounds are
918 all below 0.2 and the measured OH could be a result of peroxy radical chemistry.

919 **8 Conclusions**

920 This manuscript provides a protocol by which the central features of alkene ozonolysis chemistry can be included
921 in an explicit automatic chemical mechanism generator. It also serves to highlight the many gaps that remain in
922 our knowledge of this complex, atmospherically important, process. This will hopefully help direct both
923 experimental and theoretical research towards improving understanding in these areas. Some of the major areas
924 of uncertainty identified in this work include:

- 925
- 926 (i) The impact of oxygenated substituents on POZ fragmentation
 - 927 (ii) The impact of alkene structure on (*E*)/(*Z*)-CI conformer yields
 - 928 (iii) Products of the hot acid / ester channel and trends in the stabilisation of the hot acid / ester with size
 - 929 (iv) Further details of the mechanisms and products of non-Criegee ozonolysis chemistry, e.g. step-wise
930 decomposition of the POZ via a carbonyl hydroperoxide
 - 931 (v) Product distributions of some of the major atmospheric SCI bimolecular reactions – e.g. the reaction
932 of (*Z*)-RCHOO / CH_2OO with H_2O / $(\text{H}_2\text{O})_2$
 - 933 (vi) Experimental evidence of the products of conjugated alkene ozonolysis
 - 934 (vii) Data on OH and SCI yields from alkenes with (multiple) functional groups
- 935

936 The reliability of the protocol designed in this work was assessed using experimental values for the OH, SCI and
937 primary carbonyl yields, which are independent of the data used to derive the protocol. For these three datasets,
938 the Mean Bias Error (MBE) for the protocol based yields is below 0.05, with no substantial bias identified. The
939 protocol currently provides a fairly reliable estimate of the OH, SCI and primary carbonyl yields with Root Mean

940 Squared Errors (RMSE) of 0.12, 0.13 and 0.15, respectively. The protocol thus appears robust in representing CI
941 chemistry and its impact on atmospheric chemistry. However, the number of data available for some classes of
942 compounds remains limited, such as oxygenated, exocyclic and poly-alkenes. The errors in the yields calculated
943 for these species are also the most substantial, and additional experimental data for these categories of compound
944 would be highly valuable to improve the protocol and its assessment.

945 **Acknowledgements**

946 This work was performed as part of the MAGNIFY project, with funding from the French National Research Agency (ANR)
947 under project ANR-14-CE01-0010, and the UK Natural Environment Research Council (NERC) via grant NE/M013448/1. It
948 was also partially funded by the European Commission (EUROCHAMP-2020 (grant no. 730997)) and the UK National Centre
949 for Atmospheric Sciences (NCAS) Air Pollution Theme.

950 **Data availability**

951 All relevant data and supporting information have been provided in the Supplement.

952 **Author contribution**

953 All authors defined the scope of the work. MJN and CM-V developed and applied the SAR methods with the help of LV,
954 which were reviewed by all co-authors. MJN drafted the manuscript with the help of ARR, which was reviewed by all co-
955 authors. RV and BA tested the SAR methods in GECKO-A and carried out the statistical analysis in Section 7.

956 **Competing interests**

957 The authors declare that they have no conflict of interest.

958 **Special issue statement**

959 This article is part of the special issue “Simulation chambers as tools in atmospheric research (AMT/ACP/GMD inter-journal
960 SI)”. It is not associated with a conference.

961 **References**

- 962 Ahrens, J., Carlsson, P. T. M., Hertl, N., Olzmann, M., Pfeifle, M., Wolf, J. L., and Zeuch, T.: Infrared Detection of Criegee
963 Intermediates Formed during the Ozonolysis of β -pinene and Their Reactivity towards Sulfur Dioxide, *Angew. Chem.*, 53,
964 715–719, 2014.
- 965 Alam, M. S., Camredon, M., Rickard, A. R., Carr, T., Wyche, K. P., Hornsby, K. E., Monks, P. S., and Bloss, W. J.: Total
966 radical yields from tropospheric ethene ozonolysis, *Phys. Chem. Chem. Phys.*, 13, 11002–11015, 2011.
- 967 Almatrneh, M. H., Elayan, I. A., Altarawneh, M., and Hollett, J. W.: A computational study of the ozonolysis of sabinene,
968 *Theor. Chem. Acc.*, 138, Article No. 30, 2019.
- 969 Al Mulla, I., Viera, L., Morris, R., Sidebottom, H., Treacy, J., and Mellouki, A.: Kinetics and Mechanisms for the Reactions
970 of Ozone with Unsaturated Oxygenated Compounds, *Chem. Phys. Chem.*, 11, 4069-4078, 2010.
- 971 Anglada, J. M., Bofill, J. M., Olivella, S., and Solé, A.: Theoretical Investigation of the Low-Lying Electronic States of
972 Dioxirane: Ring Opening to Dioxymethane and Dissociation into CO₂ and H₂, *J. Phys. Chem. A*, 102, 3398–3406, 1998.
- 973 Anglada, J. M., Crehuet, R., and Bofill, J. M.: The Ozonolysis of Ethylene: A Theoretical Study of the Gas-Phase Reaction
974 Mechanism, *Chem. Eur. J.*, 5, 1809-1822, 1999.

975 Aschmann, S. M., Tuazon, E. C., Arey, J., and Atkinson, R.: Products of the Gas-Phase Reaction of O₃ with Cyclohexene, *J.*
976 *Phys. Chem. A*, 107, 2247–2255, 2003.

977 Atkinson, R. and Aschmann, S. M.: OH radical production from the gas-phase reactions of O₃ with a series of alkenes under
978 atmospheric conditions, *Environ. Sci. Technol.*, 27, 1357-1363, 1993.

979 Atkinson, R., Baulch, D. L., Cox, R. A., Crowley, J. N., Hampson, R. F., Hynes, R. G., Jenkin, M. E., Rossi, M. J., Troe, J.,
980 and IUPAC Subcommittee: Evaluated kinetic and photochemical data for atmospheric chemistry: Volume II – gas phase
981 reactions of organic species, *Atmos. Chem. Phys.*, 6, 3625–4055, <https://doi.org/10.5194/acp-6-3625-2006>, 2006.

982 Aumont, B., Szopa, S., and Madronich, S.: Modelling the evolution of organic carbon during its gas-phase tropospheric
983 oxidation: development of an explicit model based on a self generating approach, *Atmos. Chem. Phys.*, 5, 2497-2517,
984 <https://doi.org/10.5194/acp-5-2497-2005>, 2005.

985 Barber, V. P., Shubhrangshu, P., Green, A. M., Trongsiwat, N., Walsh, P. J., Klippenstein, S. J., and Lester, M. I.: Four-
986 Carbon Criegee Intermediate from Isoprene Ozonolysis: Methyl Vinyl Ketone Oxide Synthesis, Infrared Spectrum, and OH
987 Production, *J. Am. Chem. Soc.*, 140, 10866-10880, 2018.

988 Barber, V. P., Hansen, A. S., Georgievskii, Y., Klippenstein, S. J., and Lester, M. I.: Experimental and theoretical studies of
989 the doubly substituted methyl-ethyl Criegee intermediate : Infra-red action spectroscopy a unimolecular decay to OH radical
990 products, *J. Chem. Phys.*, 152, 094301, doi:10.1063/5.0002422, 2020.

991 Barnes, I., Zhou, S.M., Klotz, B.: In Final Report of the EU project MOST, Contract EVK2-CT-2001-00114. European Union,
992 Brussels, 2005.

993 Bauld, N. L., Thompson, J. A., Hudson, C. E., and Bailey, P. S.: Stereospecificity in Ozonide and Cross-Ozonide Formation,
994 *J. Am. Chem. Soc.*, 90, 1822-1830, 1968.

995 Bernard, F., Eglunent, G., Daële, V., and Mellouki, A.: Kinetics and Products of Gas-Phase Reactions of Ozone with Methyl
996 Methacrylate, Methyl Acrylate, and Ethyl Acrylate, *J. Phys. Chem. A*, 114, 8376–8383, 2010.

997 Berndt, T., Voigtländer, J., Stratmann, F., Junninen, H., Mauldin III, R. L., Sipilä, M., Kulmala, M., and Herrmann, H.:
998 Competing atmospheric reactions of CH₂OO with SO₂ and water vapour, *Phys. Chem. Chem. Phys.*, 16, 19130–19136, 2014a.

999 Berndt, T., Jokinen, T., Sipilä, M., Mauldin III, R. L., Herrmann, H., Stratmann, F., Junninen, H., and Kulmala, M.: H₂SO₄
1000 formation from the gas-phase reaction of stabilized Criegee intermediates with SO₂: Influence of water vapour content and
1001 temperature, *Atmos. Environ.*, 89, 603-612, 2014b.

1002 Berndt, T., Kaethner, R., Voigtländer, J., Stratmann, F., Pfeifle, M., Reichle, P., Sipilä, M., Kulmala, M., and Olzmann, M.:
1003 Kinetics of the unimolecular reaction of CH₂OO and the bimolecular reactions with the water monomer, acetaldehyde and
1004 acetone under atmospheric conditions, *Phys. Chem. Chem. Phys.*, 17, 19862–19873, 2015.

1005 Bey, I., Aumont, B., and Toupance, G.: The nighttime production of OH radicals in the continental troposphere, *Geophys. Res.*
1006 *Letts*, 24, 1067-1070, 1997.

1007 Cabezas, C., and Endo, Y.: Spectroscopic Characterization of the Reaction Products between the Criegee Intermediate CH₂OO
1008 and HCl, *Chem. Phys. Chem.*, 18, 1860-1863, 2017.

1009 Cabezas, C., and Endo, Y.: The reaction between the methyl Criegee intermediate and hydrogen chloride: an FTMW spectroscopic
1010 study, *Phys. Chem. Chem. Phys.*, 20, 22569-22575, 2018.

1011 Cabezas, C., and Endo, Y.: Observation of hydroperoxyethyl formate from the reaction between the methyl Criegee intermediate and
1012 formic acid, *Phys. Chem. Chem. Phys.*, 22, 446-454, 2020.

1013 Calvert, J. G., Atkinson, R., Kerr, J. A., Madronich, S., Moortgat, G. K., Wallington, T. J., and Yarwood, G.: *The Mechanism of*
1014 *Atmospheric Oxidation of the Alkenes*, Oxford University Press, New York, USA, 552 pp., 2000.

1015 Campos-Pineda, M. and Zhang, J.: Product yields of stabilized Criegee intermediates in the ozonolysis reactions of *cis*-2-
1016 butene, 2-methyl-2-butene, cyclopentene, and cyclohexene, *Science China Chemistry*, 61, 850-856, 2018.

1017 Caravan, R. L., Khan, A. H. M., Rotavera, B., Papajak, E., Antonov, I. O., Chen, M. -W., Au, K., Chao, W., Osborn, D. L.,
1018 Lin, J. J. -M., Percival, C. J., Shallcross, D. E., and Taatjes, C. E.: Products of Criegee intermediate reactions with NO₂:
1019 experimental measurements and tropospheric implications, *Faraday Discuss.*, 200, 313-330, 2017.

1020 Caravan, R. L., Vansco, M. F., Au, K., Khan, M. A. H., Li, Y. L., Winiberg, F. A., ... & Lester, M. I.: Direct kinetic
1021 measurements and theoretical predictions of an isoprene-derived Criegee intermediate. *Proceedings of the National Academy*
1022 *of Sciences*, 117(18), 9733-9740, 2020.

1023 Carr, S. A., Glowacki, D. R., Liang, C. -H., Baeza-Romero, M. T., Blitz, M. A., Pilling, M. J., and Seakins, P. W.: Experimental
1024 and Modeling Studies of the Pressure and Temperature Dependences of the Kinetics and the OH Yields in the Acetyl + O₂
1025 Reaction, *J. Phys. Chem. A.*, 115, 1069–1085, 2011.

1026 Carslaw, N.: A new detailed chemical model for indoor air pollution, *Atmos. Environ.*, 41, 1164-1179, 2007.

1027 Chang, J. -G., Chen, H. -T., Xu, S., and Lin, M. C.: Computational study on the kinetics and mechanisms for the unimolecular
1028 decomposition of formic and oxalic acids, *J. Phys. Chem. A.*, 111, 6789–6797, 2007.

1029 Chao, W., Hsieh, J. -T., Chang C.-H., and Lin J. J. -M.: Direct kinetic measurement of the reaction of the simplest Criegee
1030 intermediate with water vapour, *Science*, 347, 751–754, doi:10.1126/science.1261549, 2015.

1031 Chen, B. -Z., Anglada, J. M., Huang, M. -B., and Kong, F.: The Reaction of CH₂ (X³B₁) with O₂ (X³Σ_g⁻): A Theoretical
1032 CASSCF/CASPT2 Investigation, *J. Phys. Chem. A*, 106, 1877–1884, 2002.

1033 Chhantyal-Pun, R., Davey, A., Shallcross, D. E., Percival, C. J., and Orr-Ewing, A. J.: A kinetic study of the CH₂OO Criegee
1034 intermediate self-reaction, reaction with SO₂ and unimolecular reaction using cavity ring-down spectroscopy, *Phys. Chem.*
1035 *Chem. Phys.*, 17, 3617–3626, 2015.

1036 Chhantyal-Pun, R., Khan, M. A. H., Taatjes, C. A., Percival, C. J., Orr-Ewing, A. J., and Shallcross, D. E.: Criegee
1037 intermediates: production, detection and reactivity, *Int. Rev. Phys. Chem.*, 39, 385-424, 2020.

1038 Chung, C. -A., Su, J. W., and Lee, Y. -P.: Detailed mechanism and kinetics of the reaction of Criegee intermediate CH₂OO
1039 with HCOOH investigated *via* infrared identification of conformers of hydroperoxymethyl formate and formic acid anhydride,
1040 *Phys. Chem. Chem. Phys.*, 21, 21445–21455, 2019.

1041 Chuong, B., Zhang, J., and Donahue, N. M.: Cycloalkene Ozonolysis: Collisionally Mediated Mechanistic Branching, *J. Am.*
1042 *Chem. Soc.*, 126, 12363–12373, 2004.

1043 Cremer, D.: Stereochemistry of the Ozonolysis of Alkenes: Ozonide versus Carbonyl Oxide Control, *Angew. Chem.*, 20,
1044 888-889, 1981.

1045 Cox, R. A., Ammann, M., Crowley, J. N., Herrmann, H., Jenkin, M. E., McNeill, V. F., Mellouki, A., Troe, J., and Wallington,
1046 T. J.: Evaluated kinetic and photochemical data for atmospheric chemistry: Volume VII – Criegee intermediates, *Atmos.*
1047 *Chem. Phys.*, 20, 13497-13519, 2020.

1048 Cremer, D.: Theoretical Determination of Molecular Structure and Conformation. 8. Energetics of the Ozonolysis Reaction.
1049 Primary Ozonide vs. Carbonyl Oxide Control of Stereochemistry, *J. Am. Chem. Soc.*, 103, 3627-3633, 1981.

1050 Drozd, G. T., Kroll, J., and Donahue, N. M.: 2,3-Dimethyl-2-butene (TME) ozonolysis: Pressure dependence of stabilized
1051 criegee intermediates and evidence of stabilized vinyl hydroperoxides, *J. Phys. Chem. A*, 115, 161-166, 2011.

1052 Drozd, G. T., and Donahue, N. M.: Pressure dependence of stabilized Criegee intermediate formation from a sequence of
1053 alkenes, *J. Phys. Chem. A*, 115, 4381-4387, 2011.

1054 Drozd, G. T., Kurtén, T., Donahue, N. M., Lester, M. I.: Unimolecular decay of the dimethyl-substituted criegee intermediate
1055 in alkene ozonolysis: Decay time scales and the importance of tunnelling, *J. Phys. Chem. A*, 121, 6036-6045, 2017.

1056 Ehn, M., Thornton, J. A., Kleist, E., Sipilä, M., Junninen, H., Pullinen, I., Springer, M., Rubach, F., Tillmann, R., Lee, B.,
1057 Lopez-Hilfiker, F., Andres, S., Acir, I.-H., Rissanen, M., Jokinen, T., Schobesberger, S., Kangasluoma, J., Kontkanen, J.,
1058 Nieminen, T., Kurteín, T., Nielsen, L. B., Jørgensen, S., Kjaergaard, H. G., Canagaratna, M., Maso, M. D., Berndt, T., Petäjä,
1059 T., Wahner, A., Kerminen, V.-M., Kulmala, M., Worsnop, D. R., Wildt, J., and Mentel, T. F.: A large source of low-volatility
1060 secondary organic aerosol, *Nature*, 506, 476–479, <https://doi.org/10.1038/nature13032>, 2014.

1061 Elshorbany, Y. F., Kurtenbach, R., Wiesen, P., Lissi, E., Rubio, M., Villena, G., Gramsch, E., Rickard, A. R., Pilling, M. J.,
1062 and Kleffmann, J.: Oxidation capacity of the city air of Santiago, Chile, *Atmos. Chem. Phys.*, 9, 2257–2273,
1063 <https://doi.org/10.5194/acp-9-2257-2009>, 2009.

1064 Emmerson, K. M., Carslaw, N., and Pilling, M. J.: Urban Atmospheric Chemistry During the PUMA Campaign 2: Radical
1065 Budgets for OH, HO₂ and RO₂, *J. Atmos. Chem.*, 52, 165-183, 2005.

1066 Fenske, J. D., Hasson, A. S., Paulson, S. E., Kuwata, K. T., Ho, A., and Houk, K. N.: The Pressure Dependence of the OH
1067 Radical Yield from Ozone-Alkene Reactions, *J. Phys. Chem. A*, 104, 7821-7833, 2000.

1068 Fliszár, S., and Granger, M.: A Quantitative Investigation of the Ozonolysis Reaction: XI. On the Effects of Substituents in
1069 Directing the Ozone Cleavage of trans-1,2-Disubstituted Ethylenes, *J. Am. Chem. Soc.*, 92, 3361-3369, 1970.

1070 Fliszár, S., and J., Renard: Quantitative investigation of the ozonolysis reaction. XIV. A simple carbonium ion stabilization
1071 approach to the ozone cleavage of unsymmetrical olefins, *J. Am. Chem. Soc.*, 93, 6953-6963, 1970.

1072 Fliszár, S., J., Renard, and Simon, D. Z.: A Quantitative Investigation of the Ozonolysis Reaction. XV. Quantum Chemical
1073 Interpretation of the Substituent Effects on the Cleavage of 1,2,3-Trioxolanes, *J. Am. Chem. Soc.*, 93, 6953-6963, 1971.

1074 Foreman, E. S., Kapnas, K. M., and Murray, C.: Reactions between Criegee Intermediates and the inorganic Acids HCl and
1075 HNO₃: Kinetics and Atmospheric Implications, *Angew. Chem. Int. Ed. Engl.*, 55, doi:10.1002/anie.201604662, 2016.

1076 Grosjean, D., Williams, E. L., and Grosjean, E.: Atmospheric chemistry of isoprene and of its carbonyl products, *Environ. Sci.*
1077 *Technol.*, 27, 830–840, 1993.

1078 Grosjean, D., Williams, E. L., Grosjean, E., Andino, J. M., and Seinfeld, J. H.: Atmospheric oxidation of biogenic
1079 hydrocarbons: reaction of ozone with b-pinene, d-limonene and trans-caryophyllene, *Environ. Sci. Technol.*, 27, 2754–2758,
1080 1993.

1081 Grosjean, D., Grosjean, E., and Williams, E. L.: Atmospheric Chemistry of Olefins: A Product Study of the Ozone-Alkene
1082 Reaction with Cyclohexane Added to Scavenge OH, *Environ. Sci. Technol.*, 28, 188–196, 1994.

1083 Grosjean, E., Grosjean, D., and Seinfeld, J. H.: Gas phase reaction of ozone with trans-2-hexenal, trans-2-hexenyl acetate,
1084 ethylvinyl ketone and 6-methyl-5-hepten-2-one, *Int. J. Chem. Kinet.*, 28, 373–382, 1996.

1085 Grosjean, E., and Grosjean, D.: Carbonyl products of the gas phase reaction of ozone with 1,1-disubstituted alkenes. *J. Atmos.*
1086 *Chem.*, 24, 141–156, <https://doi.org/10.1007/BF00162408>, 1996a.

1087 Grosjean, E. and Grosjean, D.: Rate constants for the gas phase reaction of ozone with 1,1-disubstituted alkenes, *Int. J. Chem.*
1088 *Kinet.*, 28, 911–918, 1996b.

1089 Grosjean, E. and Grosjean, D.: Gas phase reaction of alkenes with ozone: Formation yields of primary carbonyls and
1090 biradicals. *Environ. Sci. Technol.*, 31(8), 2421-2427, 1997a.

1091 Grosjean, E., and Grosjean, D.: The Gas Phase Reaction of Unsaturated Oxygenates with Ozone: Carbonyl Products and
1092 Comparison with the Alkene-Ozone Reaction, *J. Atmos. Chem.*, 27, 271-289, 1997b.

1093 Grosjean, E., and Grosjean, D.: The Reaction of Unsaturated Aliphatic Oxygenates with Ozone, *J. Atmos. Chem.*, 32, 205-
1094 232, 1999.

1095 Gutbrod, R., Meyer, S., Rahman, M. M., and Schindler, R. N.: On the use of CO as scavenger for OH radicals in the ozonolysis
1096 of simple alkenes and isoprene, *Int. J. Chem. Kinet.*, 29, 717-723, 1997.

1097 Hakala, J. P., and Donahue, N. M.: Pressure-Dependent Criegee Intermediate Stabilization from Alkene Ozonolysis, *J. Phys.*
1098 *Chem. A*, 120, 2173-2178, 2016.

1099 Hakala, J. P., and Donahue, N. M.: Pressure Stabilization of Criegee Intermediates Formed from Symmetric trans-Alkene
1100 Ozonolysis, *J. Phys. Chem. A*, 122, 9426-9434, 2018.

1101 Hakola, H., Arey, J., Aschmann, S. M., and Atkinson, R.: Product formation from the gas-phase reactions of OH radicals and
1102 O₃ with a series of monoterpenes, *J. Atmos. Chem.*, 18, 75-102, 1994.

1103 Hansel, A., Scholz, W., Mentler, B., Fischer, L., and Berndt, T.: Detection of RO₂ radicals and other products from
1104 cyclohexene ozonolysis with NH₄⁺ and acetate chemical ionization mass spectrometry, *Atmospheric Environment*, 186, 248-
1105 255, <https://doi.org/10.1016/j.atmosenv.2018.04.023>, 2018.

1106 Hasson, A. S., Orzechowska, G., and Paulson, S. E.: Production of stabilized Criegee intermediates and peroxides in the gas
1107 phase ozonolysis of alkenes 1. Ethene, trans-2-butene, and 2,3- dimethyl-2-butene, *J. Geophys. Res.*, 106, 34131–34142,
1108 2001a.

1109 Hasson, A. S., Ho, A. W., Kuwata, K., and Paulson, S. E.: Production of stabilized Criegee intermediates and peroxides in the
1110 gas phase ozonolysis of alkenes 2. Asymmetric and biogenic alkenes, *J. Geophys. Res.*, 106, 34143–34153, 2001b.

1111 Hatakeyama, S., Kobayashi, H., and Akimoto, H.: Gas-phase oxidation of sulfur dioxide in the ozone-olefin reactions, *J. Phys.*
1112 *Chem.* 88, 4736-4739, 1984.

1113 Heard, D. E., Carpenter, L. J., Creasey, D. J., Hopkins, J. R., Lee, J. R., Lewis, A. C., Pilling, M. J., Seakins, P. W., Carslaw,
1114 N., and Emmerson, K. M.: High levels of the hydroxyl radical in the winter urban troposphere, *Geophys. Res. Lett.*, 31,
1115 L18112, 2004.

1116 Herron, J. T., and Huie, R. E. Stopped-flow studies of the mechanisms of ozone-alkene reactions in the gas phase: propene
1117 and isobutene, *J. Am. Chem. Soc.*, 99, 5430-5435, 1977.

1118 Herron, J. T., and Huie, R. E. Stopped-flow studies of the mechanisms of ozone-alkene reactions in the gas phase. I. Ethylene,
1119 *J. Am. Chem. Soc.*, 99, 5430-5435, 1978.

1120 Huang, H. -L., Chao, W., and Lin, J. J. -M.: Kinetics of a Criegee intermediate that would survive at high humidity and may
1121 oxidize atmospheric SO₂, *Proc. Natl. Acad. Sci.*, 112, 10857–10862, 2015.

1122 Iyer, S., Rissanen, M. P., Valiev, R., Barua, S., Krechmer, J. E., Thornton, J., Ehn, M., and Kurtén, T.: Molecular mechanism
1123 for rapid autoxidation in α -pinene ozonolysis, *Nat. Comms.*, 12, doi.org/10.1038/s41467-021-21172-w, 2021.

1124 Jenkin, M. E., Saunders, S. M., and Pilling, M. J.: The tropospheric degradation of volatile organic compounds: a protocol for
1125 mechanism development, *Atmos. Environ.*, 31, 81–104, 1997.

1126 Jenkin, M. E., Young, J. C., and Rickard, A. R.: The MCM v3.3.1 degradation scheme for isoprene, *Atmos. Chem. Phys.*, 15,
1127 11433-11459, 2015.

1128 Jenkin, M. E., Valorso, R., Aumont, B., Rickard, A. R., and Wallington, T. J.: Estimation of rate coefficients and branching
1129 ratios for gas-phase reactions of OH with aliphatic organic compounds for use in automated mechanism construction, *Atmos.*
1130 *Chem. Phys.*, 18, 9297–9328, <https://doi.org/10.5194/acp-18-9297-2018>, 2018a.

1131 Jenkin, M. E., Valorso, R., Aumont, B., Rickard, A. R., and Wallington, T. J.: Estimation of rate coefficients and branching
1132 ratios for gas-phase reactions of OH with aromatic organic compounds for use in automated mechanism construction, *Atmos.*
1133 *Chem. Phys.*, 18, 9329–9349, <https://doi.org/10.5194/acp-18-9329-2018>, 2018b.

1134 Jenkin, M. E., Valorso, R., Aumont, B., and Rickard, A. R.: Estimation of rate coefficients and branching ratios for reactions
1135 of organic peroxy radicals for use in automated mechanism construction, *Atmos. Chem. Phys.*, 19, 7691–7717,
1136 <https://doi.org/10.5194/acp-19-7691-2019>, 2019.

1137 Jenkin, M. E., Valorso, R., Aumont, B., Newland, M. J., and Rickard, A. R.: Estimation of rate coefficients for the reactions
1138 of O₃ with unsaturated organic compounds for use in automated mechanism construction, *Atmos. Chem. Phys.*, 20, 12921-
1139 12937, 2020.

1140 Johnson, D. and Marston, G.: The gas-phase ozonolysis of unsaturated volatile organic compounds in the troposphere, *Chem.*
1141 *Soc. Rev.*, 37, 699–716, 2008.

1142 Kalalian, C., Roth, E., El Dib, G., Singh, H. J., Rao, P. K., and Chakir, A.: Product investigation of the gas phase ozonolysis
1143 of 1-penten-3-ol, *cis*-2-penten-1-ol and *trans*-3-hexen-1-ol, *Atmos. Environ.*, 238, 117732, 2020.

1144 Kalberer, M., Yu, J., Cocker, D. R., Flagan, R. C., and Seinfeld, J. H.: Aerosol Formation in the Cyclohexene-Ozone System,
1145 *Environ. Sci. Technol.*, 34, 4894-4901, 2000.

1146 Kidwell, N. M., Li, H., Wang, X., Bowman, J. M., and Lester, M. I.: Unimolecular dissociation dynamics of vibrationally
1147 activated CH₃CHOO Criegee intermediates to OH radical products, *Nat. Chem.*, 8, 509-514, 2016.

1148 Klotz, B., Barnes, I., and Imamura, T.: Product study of the gas phase reactions of O₃, OH and NO₃ reactions with methyl
1149 vinyl ether, *Phys. Chem. Chem. Phys.*, 6, 1725–1734, 2004.

1150 Kristensen, K., Cui, T., Zhang, H., Gold, A., Glasius, M., and Surratt, J. D.: Dimers in α -pinene secondary organic aerosol:
1151 effect of hydroxyl radical, ozone, relative humidity and aerosol acidity, *Atmos. Chem. Phys.*, 14, 4201–4218, 2014.

1152 Kroll, J. H., Hanisco, T. F., Donahue, N. M., Demerjian, K. L., and Anderson, J. G.: Accurate, direct measurements of OH
1153 yields from gas-phase ozone-alkene reactions using an in-situ LIF instrument, *Geophys. Res. Lett.*, 28, 3863-3866, 2001.

1154 Kroll, J., Donahue, N. M., Cee, V. J., Demerjian, K. L., and Anderson, J. G.: Gas-phase ozonolysis of alkenes: Formation of
1155 OH from anti carbonyl oxides, *J. Am Chem. Soc.*, 124, 8518-8519, 2002.

1156 Kuwata, K. T., Valin, L. C., and Converse, A. D.: Quantum chemical and master equation studies of the methyl vinyl carbonyl
1157 oxides formed in isoprene ozonolysis, *J. Phys. Chem. A*, 109, 10710-10725, 2005.

1158 Kuwata, K. T., and Valin, L. C.: Quantum chemical and RRKM/master equation studies of isoprene ozonolysis: Methacrolein
1159 and methacrolein oxide, *Chem. Phys. Lett.*, 451, 186-191, 2008.

1160 Kuwata, K. T., Guinn, E. J., Hermes, M. R., Fernandez, J. A., Mathison, J. M., and Huang, K. A.: Computational Re-
1161 examination of the Criegee Intermediate-Sulfur Dioxide Reaction, *J. Phys. Chem. A*, 119, 10316-10335, 2015.

1162 Kuwata, K. T., Luu, L., Weberg, A. B., Huang, K., Parsons, A. J., Peebles, L. A., Rackstraw, N. B., and Kim, M. J.: Quantum
1163 Chemical and Statistical Rate Theory Studies of the Vinyl Hydroperoxides Formed in *trans*-2-Butene and 2,3-Dimethyl-2-
1164 butene Ozonolysis, *J. Phys. Chem. A*, 122, 2485-2502, 2018.

1165 Lee, A., Goldstein, A. H., Keywood, M. D., Gao, S., Varutbangkul, V., Bahreini, R., Ng, N. L., Flagan, R. C., and Seinfeld, J.
1166 H.: Gas-phase products and secondary organic aerosol yields from the ozonolysis of ten different terpenes, *J. Geophys. Res.*,
1167 111, D07302, 2006.

1168 Le Person, A., Solignac, G., Oussar, F., Daële, V., Mellouki A., Winterhalter, R., and Moortgat, G. K.: Gas phase reaction of
1169 allyl alcohol (2-propen-1-ol) with OH radicals and ozone, *Phys. Chem. Chem. Phys.*, 11, 7619–7628, 2009.

1170 Lei, X., Wang, W., Gao, J., Wang, S. and Wang, W.: Atmospheric Chemistry of Enols: The Formation Mechanisms of Formic
1171 and Peroxyformic Acids in Ozonolysis of Vinyl Alcohol, *J. Phys. Chem. A*, 124, 4271-4279, 2020.

1172 Lewin, A. G., Johnson, D., Price, D. W., and Marston, G.: Aspects of the kinetics and mechanism of the gas-phase reactions
1173 of ozone with conjugated dienes, *Phys. Chem. Chem. Phys.*, 3, 1253–1261, 2001.

1174 Lewis, T. R., Blitz, M. A., Heard, D. E., and Seakins, P. W. Direct evidence for a substantive reaction between the Criegee
1175 intermediate, CH₂OO, and the water vapour dimer, *Phys. Chem. Chem. Phys.*, 17, 4859–4863, 2015.

1176 Lin, L.-C., Chang, H., Chang, C., Chao, W., Smith, M. C., Chang, C., Lin, J. J., and Takahashi, K. Competition between H₂O
1177 and (H₂O)₂ reactions with CH₂OO/CH₃CHOO, *Phys. Chem. Chem. Phys.*, 18, 4557–4568, 2016.

1178 Long, B., Bao, J. L., and Truhlar, D. G.: Rapid unimolecular reaction of stabilized Criegee intermediates and implications for
1179 atmospheric chemistry, *Nat. Commun.*, 10, doi:10.1038/s41467-019-09948-7, 2019.

1180 Ma, Y., and Marston G.: Multifunctional acid formation from the gas-phase ozonolysis of β-pinene, *Phys. Chem. Chem. Phys.*,
1181 10, 6115–6126, 2008.

1182 Ma, Y., and Marston G.: Formation of organic acids from the gas-phase ozonolysis of terpinolene, *Phys. Chem. Chem. Phys.*,
1183 11, 4198–4209, 2009.

1184 Martinez, R. I. and Herron, J. T.: Stopped-flow studies of the mechanisms of alkene-ozone reactions in the gas-phase:
1185 tetramethylethylene, *J. Phys. Chem. A*, 91, 946–953, 1987.

1186 Mauldin III, R. L., Berndt, T., Sipilä, M., Paasonen, P., Petäjä, T., Kim, S., Kurtén, T., Stratmann, F., Kerminen, V.-M., and
1187 Kulmala, M.: A new atmospherically relevant oxidant of sulphur dioxide, *Nature*, 488, 193–196, doi:10.1038/nature11278,
1188 2012.

1189 Neeb, P., Horie, O., and Moortgat, G. K. The nature of the transitory product in the gas-phase ozonolysis of ethene, *Chem.*
1190 *Phys. Lett.*, 37, 150-156, 1995.

1191 Neeb, P., Horie, O., and Moortgat, G. K. Formation of secondary ozonides in the gas-phase ozonolysis of simple alkenes,
1192 *Tetrahedron Lett.*, 246, 9297-9300, 1996.

1193 Neeb, P., Sauer, F., Horie, O., and Moortgat, G. K. Formation of hydroxymethyl hydroperoxide and formic acid
1194 in alkene ozonolysis in the presence of water vapour, *Atmos. Environ.*, 31, 1417-1423, 1997.

1195 Newland, M. J., Rickard, A. R., Alam, M. S., Vereecken, L., Muñoz, A., Ródenas, M., and Bloss, W. J.: Kinetics of stabilised
1196 Criegee intermediates derived from alkene ozonolysis: reactions with SO₂, H₂O and decomposition under boundary layer
1197 conditions, *Phys. Chem. Chem. Phys.*, 17, 4076-4088, 2015.

1198 Newland, M. J., Rickard, A. R., Sherwen, T., Evans, M. J., Vereecken, L., Muñoz, A., Ródenas, M., and Bloss, W. J.: The
1199 atmospheric impacts of monoterpene ozonolysis on global stabilised Criegee intermediate budgets and SO₂ oxidation:
1200 experiment, theory and modelling, *Atmos. Chem. Phys.*, 18, 6095-6120, 2018.

1201 Newland, M. J., Nelson B. S., Muñoz, A., Ródenas, M., Vera, T., Tarrega, J., and Rickard, A. R.: Trends in stabilisation of
1202 Criegee intermediates from alkene ozonolysis, *Phys. Chem. Chem. Phys.*, 22, 13698-13706, 2020.

1203 Nguyen, T. L., Winterhalter, R., Moortgat, G., Kanawati, B., Peeters, J., and Vereecken, L.: The gas-phase ozonolysis of β -
1204 caryophyllene (C₁₅H₂₄). Part II: A theoretical study, *Phys. Chem. Chem. Phys.*, 11, 4173-4183, 2009a.

1205 Nguyen, T. L., Peeters, J., and Vereecken, L.: Theoretical study of the gas-phase ozonolysis of β -pinene (C₁₀H₁₆), *Phys. Chem.*
1206 *Chem. Phys.*, 11, 5643-5656, 2009b.

1207 Nguyen, T. L., Lee, H., Matthews, D. A., McCarthy, M. C., and Stanton, J. F.: Stabilization of the Simplest Criegee
1208 Intermediate from the Reaction between Ozone and Ethylene: A High-Level Quantum Chemical and Kinetic Analysis of
1209 Ozonolysis, *J. Phys. Chem. A*, 119, 5524–5533, 2015.

1210 Nguyen, T. B., Tyndall, G. S., Crounse, J. D., Teng, A. P., Bates, K. H., Schwantes, R. H., Coggon, M. M., Zhang, L., Feiner,
1211 P., and Miller, D. O.: Atmospheric fates of Criegee intermediates in the ozonolysis of isoprene, *Phys. Chem. Chem. Phys.*, 18,
1212 10241– 10254, 2016.

1213 Niki, H., Maker, P. D., Savage, C. M., Breitenbach, L. P., and Hurley, M. D. FTIR spectroscopic study of the mechanism for
1214 the gas-phase reaction between ozone and tetramethylethylene, *J. Phys. Chem. A*, 91, 941–946, 1987.

1215 O’Dwyer, M. A., Carey, T. J., Healy, R. M., Wenger, J. C., Picquet-Varrault, B., and Doussin, J. F.: The Gas-phase Ozonolysis
1216 of 1-Penten-3-ol, (Z)-2-Penten-1-ol, and 1-Penten-3-one: Kinetics, Products and Secondary Organic Aerosol Formation, *Z.*
1217 *Phys. Chem.*, 224, 1059–1080, 2010.

1218 O’Neal, H. E., and Blumstein, C.: A new mechanism for gas phase ozone-olefin reactions, *Int. J. Chem. Kinet.*, 5, 397-413,
1219 1973.

1220 Olzmann, M., Kraka, E., Cremer, D., Gutbrod, R., and Anderson, S.: Energetics, Kinetics, and Product Distributions of the
1221 Reactions of Ozone with Ethene and 2,3-Dimethyl-2-butene, *J. Phys. Chem. A*, 101, 9421–9429, 1997.

1222 Orzechowska, G. E., and Paulson, S. E.: Production of OH radicals from the reactions of C₄-C₆ internal alkenes and styrenes
1223 with ozone in the gas phase, *Atmos. Environ.*, 36, 571-581, 2002.

1224 Ouyang, B., McLeod, M. W., Jones, R. L., and Bloss, W. J.: NO₃ radical production from the reaction between the Criegee
1225 intermediate CH₂OO and NO₂, *Phys. Chem. Chem. Phys.*, 15, 17070-17075, 2013.

1226 Paulson, S. E., and Orlando, J. J. The reactions of ozone with alkenes: An important source of HO_x in the boundary layer,
1227 *Geophys. Res. Letts.*, 23, 3727-3730, 1996.

1228 Peltola, J., Seal, P., Inkilä, A., and Eskola, A.: Time-resolved, broadband UV-absorption spectrometry measurements of
1229 Criegee intermediate kinetics using a new photolytic precursor: unimolecular decomposition of CH₂OO and its reaction with
1230 formic acid, *Phys. Chem. Chem. Phys.*, 22, 11797-11808, 2020.

1231 Percival, C. J., Welz, O., Eskola, A. J., Savee, J. D., Osborn, D. L., Topping, D. O., Lowe, D., Utembe, S. R., Bacak, A.,
1232 McFiggans, G., Cooke, M. C., Xiao, P., Archibald, A. T., Jenkin, M. E., Derwent, R. G., Riipinen, I., Mok, D. W. K., Lee, E.
1233 P. F., Dyke, J. M., Taatjes, C. A., and Shallcross, D. E.: Regional and global impacts of Criegee intermediates on atmospheric
1234 sulphuric acid concentrations and first steps of aerosol formation, *Faraday Discuss.*, 165, 45–
1235 73, <https://doi.org/10.1039/C3FD00048F>, 2013.

1236 Pfeifle, M., Ma, Y. -T., Jasper, A. W., Harding, L. B., Hase, W. L., and Klippenstein, S. J.: Nascent energy distribution of the
1237 Criegee intermediate CH₂OO from direct dynamics calculations of primary ozonide dissociation, *J. Chem. Phys.*, 148, 174306,
1238 2018.

1239 Picquet-Varrault, B., Scarfoglierio, M, and Doussin, J. -F.: Atmospheric Reactivity of Vinyl Acetate: Kinetic and Mechanistic
1240 Study of Its Gas-Phase Oxidation by OH, O₃, and NO₃, *Environ. Sci. Technol.*, 44, 4615–4621, 2010.

1241 Pierce, J. R., Evans, M. J., Scott, C. E., D'Andrea, S. D., Farmer, D. K., Swietlicki, E., and Spracklen, D. V.: Weak global
1242 sensitivity of cloud condensation nuclei and the aerosol indirect effect to Criegee + SO₂ chemistry, *Atmos. Chem. Phys.*, 13,
1243 3163–3176, <https://doi.org/10.5194/acp-13-3163-2013>, 2013.

1244 Pinelo, L., Gudmundsdottir, A. D., and Ault, B. S.: Matrix Isolation Study of the Ozonolysis of 1,3- and 1,4-Cyclohexadiene:
1245 Identification of Novel Reaction Pathways, *J. Phys. Chem. A*, 117, 4174–4182, 2013.

1246 Raghunath, P., Lee, Y. -P., Lin, M. C.: Computational chemical kinetics for the reaction of Criegee intermediate CH₂OO with
1247 HNO₃ and its catalytic conversion to OH and HCO, *J. Phys. Chem. A*, 121, 3871–3878, 2017.

1248 Rathman, W. C. D., Claxton, T. A., Rickard, A. R., Marston, G. A theoretical investigation of OH formation in the gas-phase
1249 ozonolysis of *E*-but-2-ene and *Z*-but-2-ene, *Phys. Chem. Chem. Phys.*, 1, 3981-3985, 1999.

1250 Reissell, A., Harry, C., Aschmann, S. M., Atkinson, R., and Arey, J.: Formation of acetone from the OH radical- and O₃-
1251 initiated reactions of a series of monoterpenes, *J. Geophys. Res.*, 104, 13869–13879, 1999.

1252 Rickard, A. R., Johnson, D., McGill, C. D., and Marston, G. OH Yields in the Gas-Phase reactions of Ozone with Alkenes, *J.*
1253 *Phys. Chem. A*, 103, 7656–7664, 1999.

1254 Sakamoto, Y., Inomata, S., and Hirokawa, J.: Oligomerization Reaction of the Criegee Intermediate Leads to Secondary
1255 Organic Aerosol Formation in Ethylene Ozonolysis, *J. Phys. Chem. A*, 117, 12912–12921, 2013.

1256 Saunders, S. M., Jenkin, M. E., Derwent, R. G., and Pilling, M. J.: Protocol for the development of the Master Chemical
1257 Mechanism, MCM v3 (Part A): Tropospheric degradation of non-aromatic volatile organic compounds, *Atmos. Chem. Phys.*,
1258 3, 161-180, 2003.

1259 Sheps, L., Scully, A. M., and: UV absorption probing of the conformer-dependent reactivity of a Criegee intermediate
1260 CH₃CHOO *Phys. Chem. Chem. Phys.*, 16, 26701-26706, 2014.

1261 Sheps, L., Rotavera, B., Eskola, A. J., Osborn, D. L., Taatjes, C., Au, K., Shallcross, D. E., Khan, M. A. H., Percival, C. J.
1262 The reaction of Criegee intermediate CH₂OO with water dimer: Primary products and atmospheric impact, *Phys. Chem. Chem.*
1263 *Phys.*, 19, 21970-21979, 2017.

1264 Sipilä, M., Jokinen, T., Berndt, T., Richters, S., Makkonen, R., Donahue, N. M., Mauldin III, R. L., Kurtén, T., Paasonen, P.,
1265 Sarnela, N., Ehn, M., Junninen, H., Rissanen, M. P., Thornton, J., Stratmann, F., Herrmann, H., Worsnop, D. R., Kulmala, M.,
1266 Kerminen, V.-M., and Petäjä, T.: Reactivity of stabilized Criegee intermediates (sCIs) from isoprene and monoterpene
1267 ozonolysis toward SO₂ and organic acids, *Atmos. Chem. Phys.*, 14, 12143-12153, 2014.

1268 Smith, M. C., Chao, W., Takahashi, K., Boering, K. A., and Lin, J. J. -M.: Unimolecular Decomposition Rate of the Criegee
1269 Intermediate (CH₃)₂COO Measured Directly with UV Absorption Spectroscopy, *J. Phys. Chem. A*, doi:
1270 10.1021/acs.jpca.5b12124, 2016.

1271 Stephenson, T. A., and Lester, M. I.: Unimolecular decay dynamics of Criegee intermediates: Energy-resolved rates, thermal
1272 rates, and their atmospheric impact, *Int. Rev. Phys. Chem.*, 39, 1-33, 2020.

1273 Stone, D., Blitz, M., Daubney, L., Howes, N. U. M., and Seakins, P.: Kinetics of CH₂OO reactions with SO₂, NO₂, NO, H₂O,
1274 and CH₃CHO as a function of pressure, *Phys. Chem. Chem. Phys.*, 16, 1139–1149, 2014.

1275 Stone, D., Au, K., Sime, S., Medeiros, D. J., Blitz, M., Seakins, P., Decker, Z., and Sheps, L.: Unimolecular decomposition
1276 kinetics of the stabilised Criegee intermediates CH₂OO and CD₂OO, *Phys. Chem. Chem. Phys.*, 20, 24940–24954, 2018.

1277 Taatjes, C. A., Welz, O., Eskola, A. J., Savee, J. D., Scheer, A. M., Shallcross, D. E., Rotavera, B., Lee, E. P. F., Dyke, J. M.,
1278 Mok, D. K. W., Osborn, D. L., and Percival, C. J.: Direct Measurements of Conformer-Dependent Reactivity of the Criegee
1279 Intermediate CH₃CHOO, *Science*, 340, 177–180, 2013.

1280 Taatjes, C. A., Caravan, R. L., Winiberg, F. A. F., Zuraski, K., Au, K., Sheps, L., Osborn, D. L., Vereecken, L., and Percival,
1281 C. J.: Insertion products in the reaction of carbonyl oxide Criegee intermediates with acids: Chloro(hydroperoxy)methane
1282 formation from reaction of CH₂OO with HCl and DCl, *Mol. Phys.*, 119, e1975199,
1283 <https://doi.org/10.1080/00268976.2021.1975199>, 2021.

1284 Tadayon S. V., Foreman, E. S., and Murray, C.: Kinetics of the reactions between the Criegee intermediate CH₂OO and
1285 alcohols, *J. Phys. Chem. A*, 122, 258-268, 2018.

1286 Thiault, G., Thévenet, R., Mellouki, A., and Le Bras, G.: OH and O₃-initiated oxidation of ethyl vinyl ether, *Phys. Chem.*
1287 *Chem. Phys.*, 4, 613-619, 2002.

1288 Tuazon, E. C., Aschmann, S. M., Arey, J., and Atkinson, R.: Products of the Gas-Phase Reactions of O₃ with a Series of
1289 Methyl-Substituted Ethenes, *Environ. Sci. Technol.*, 31, 10, 3004–3009, 1997.

1290 Vansco, M. F., Caravan, R. L., Zuraski, K., Winiberg, F. A. F., Au, K., Trongsirivat, N., Walsh, P. J., Osborn, D. L. Percival,
1291 C. J., Khan, M. A. H., Shallcross, D. E., Taatjes, C. A., and Lester, M. I.: Experimental Evidence of Dioxole Unimolecular
1292 Decay Pathway for Isoprene-Derived Criegee Intermediates, *J. Phys. Chem. A*, 124, 3542-3554, 2020.

1293 Vereecken, L., and Francisco, J. S.: Theoretical studies of atmospheric reaction mechanisms in the troposphere, *Chem. Soc.*
1294 *Rev.*, 41, 6259-6293, 2012.

1295 Vereecken, L., Novelli, A., and Taraborrelli, D.: Unimolecular decay strongly limits the atmospheric impact of Criegee
1296 intermediates, *Phys. Chem. Chem. Phys.*, 19, 31599–31612, 2017.

1297 Vereecken, L.: The reaction of Criegee intermediates with acids and enols, *Phys. Chem. Chem. Phys.*, 19, 28630-28640, 2017.

1298 Vereecken, L., and Nguyen, H. M. T.: Theoretical Study of the Reaction of Carbonyl Oxide with Nitrogen Dioxide: CH₂OO
1299 + NO₂, *Int. J. Chem. Kinet.*, 49, 752-760, 2017.

1300 Vereecken, L., Aumont, B., Barnes, I., Bozzelli, J., Goldman, M., Green, W., Madronich, S., McGillen, M., Mellouki, A.,
1301 Orlando, J., Picquet-Varrault, B., Rickard, A., Stockwell, W., Wallington, T., and Carter, W.: Perspective on Mechanism
1302 Development and Structure-Activity Relationships for Gas-Phase Atmospheric Chemistry. *Int. J. Chem. Kinet.*, 50, 435-469,
1303 <https://doi-org.insu.bib.cnrs.fr/10.1002/kin.21172>, 2018.

1304 Vichiatti, R. M., Keidel Spada, R. F., Ferreira da Silva, A. B., Correto Machado, F. B., and Andrade Haiduke, R. L.: Accurate
1305 Calculations of Rate Constants for the Forward and Reverse H₂O + CO ↔ HCOOH Reactions, *Chemistry Select*, 2, 7267-
1306 7272, 2017.

1307 Viero, L.: Kinetics and mechanisms for the oxidation of unsaturated organic acids and esters under atmospheric conditions,
1308 Ph.D. Thesis, University College Dublin, 2008.

1309 Wadt, W. R., and Goddard, W. A.: The electronic structure of the Criegee intermediate. Ramifications for the mechanism of
1310 ozonolysis, *J. Am. Chem. Soc.*, 97, 3004-3021, 1975.

1311 Wang, J., Zhou, L., Wang, W., and Ge, M.: Gas-phase reaction of two unsaturated ketones with atomic Cl and O₃: kinetics
1312 and products, *Phys. Chem. Chem. Phys.*, 17, 12000–12012, 2015.

1313 Wang, S., Newland, M.J., Deng, W., Rickard, A.R., Hamilton, J.F., Muñoz, A., Ródenas, M., Vázquez, M.M., Wang, L. and
1314 Wang, X.: Aromatic photo-oxidation, a new source of atmospheric acidity, *Environmental Science & Technology*, 54, 7798-
1315 7806, 2020.

1316 Watson N. A. I., Black, J. A., Stonelake, T. M., Knowles, P. J., Beames, J. M.: An extended computational study of Criegee
1317 intermediate-alcohol reactions, *J. Phys. Chem. A*, 123, 218-229, 2019.

1318 Watson, N. A. I.: An Analysis of the Sources and Sinks for Criegee Intermediates: An Extended Computational Study, Ph.D.
1319 Thesis, University of Cardiff, <http://orca.cardiff.ac.uk/id/eprint/144742>, October 2021.

1320 Weidman, J. D., Allen, R. T., Moore, K. B., and Schaefer, H. F.: High-level theoretical characterization of the vinyloxy radical
1321 ($\cdot\text{CH}_2\text{CHO}$) + O₂ reaction. *J. Chem. Phys.*, 148, 184308, 2018.

1322 Welz, O., Savee, J. D., Osborn, D. L., Vasu, S. S., Percival, C. J., Shallcross, D. E., and Taatjes, C. A.: Direct Kinetic
1323 Measurements of Criegee Intermediate (CH₂OO) Formed by Reaction of CH₂I with O₂, *Science*, 335, 204–207, 2012.

1324 Welz, O., Eskola, A. J., Sheps, L., Rotavera, B., Savee, J. D., Scheer, A. M., Osborn, D. L., Lowe, D., Murray Booth, A., Xiao,
1325 P., Anwar H., Khan, M., Percival, C. J., Shallcross, D. E., and Taatjes, C. A.: Rate coefficients of C1 and C2 Criegee
1326 intermediate reactions with formic and acetic acid near the collision limit: direct kinetics measurements and atmospheric
1327 implications, *Angew. Chem. Int. Ed. Engl.*, 53, 4547–4750, 2014.

1328 Winterhalter, R., Neeb, P., Grossmann, D., Kolloff, A., Horie, O. and Moortgat, G.: Products and mechanism of the gas phase
1329 reaction of ozone with β -pinene. *Journal of Atmospheric Chemistry*, 35(2), 165-197, 2000.

1330 Winterhalter, R., Herrmann, F., Kanawati, B., Nguyen, T. L., Peeters, J., Vereecken, L., and Moortgat, G.: The gas-phase
1331 ozonolysis of β -caryophyllene ($C_{15}H_{24}$). Part I: an experimental study, *Phys. Chem. Chem. Phys.*, 11, 4152-4172, 2009.

1332 Wennberg, P. O., Bates, K. H., Crounse, J. D., Dodson, L. G., McVay, R. C., Mertens, L. A., Nguyen, T. B., Praske, E.,
1333 Schwantes, R. H., and Smarte, M. D.: Gas-phase reactions of isoprene and its major oxidation products, *Chem. Rev.*, 118,
1334 3337–3390, <https://doi.org/10.1021/acs.chemrev.7b00439>, 2018.

1335 Wolff, S., Boddenberg, A., Thamm, J., Turner, W. V., and Gräß, S. Gas-phase ozonolysis of ethene in the presence of carbonyl-
1336 oxide scavengers, *Atmos. Environ.*, 31, 2965-2969, 1997.

1337 Yu, J. Z., Cocker, D. R., Griffin, R. J., Flagan, R. C., and Seinfeld, J. H.: Gas-phase ozone oxidation of monoterpenes: Gaseous
1338 and particulate products, *J. Atmos. Chem.*, 34, 207–258, 1999.

1339 Zhao, Y., Wingen, L. M., Perraud, V., Greaves, J., and Finlayson-Pitts, B. J.: Role of the reaction of stabilized Criegee
1340 intermediates with peroxy radicals in particle formation and growth in air, *Phys. Chem. Chem. Phys.*, 17, 12500–12514, 2015.

1341 Zhou, S., Barnes, I., Zhu, T., Klotz, B., Albu, M., Bejan, I., and Benter, T.: Product Study of the OH, NO₃, and O₃ Initiated
1342 Atmospheric Photooxidation of Propyl Vinyl Ether, *Environ. Sci., Technol.*, 2006.

1343 Zhou, S.: Atmospheric Oxidation of Vinyl Ethers, PhD thesis, Bergische Universität Wuppertal, 2007.

1344 Ziemann, P. J.: Evidence for Low-Volatility Diacyl Peroxides as a Nucleating Agent and Major Component of Aerosol Formed
1345 from Reactions of O₃ with Cyclohexene and Homologous Compounds, *J. Phys. Chem. A*, 106, 4390–4402, 2002.

1346